ICE, BEDLOAD TRANSPORT, AND CHANNEL MORPHOLOGY

ON THE UPPER KUPARUK RIVER

By

Jeffrey A. Oatley

RECOMMENDED:

_____

_____

_____
Advisory Committee Chair

_____
Chair, Department of Civil and
Environmental Engineering

APPROVED:

_____
Dean, College of Science, Engineering, and Mathematics

_____
Dean of the Graduate School

_____
Date

ICE, BEDLOAD TRANSPORT, AND CHANNEL MORPHOLOGY ON THE UPPER KUPARUK RIVER

A

THESIS

Presented to the Faculty

Of the University of Alaska Fairbanks

In Partial Fulfillment of the Requirements

For the Degree of

MASTER OF SCIENCE

By

Jeffrey A. Oatley, B.A., M.S.

Fairbanks, Alaska

December 2002

Abstract

The objective of this study was to quantify the impact of bottom ice on sedimentation processes at a study site on the Upper Kuparuk River, in Northern Alaska. The approach taken was to use the Meyer-Peter and Mueller (1948) and Parker (1990) equations to determine bedload rating curves at four cross sections within the study reach, and to apply these rating curves to the ten year flow history of the study site to determine the total potential bedload transport that was suppressed during snowmelt runoff. In conjunction with this analysis, a tracer rock study was performed at the study site. During the first two years of the project, the field study yielded little bedload transport information, as there were no competent flows during this time. However, the storm of record occurred in August of 2002, which provided an opportunity to observe the geomorphic response to a major event, to estimate an average bedload transport rate based on the virtual velocity of the recovered tracer rocks, and to compare the predictive methods to the tracer data based calculations. The results suggest that the potential bedload transport (500 m^3) over the ten-year flow history is comparable to the amount of transport that occurred during the extreme event of August 2002 (870 m^3), and that the suppression of bedload transport, due to an ice covered bed surface, likely affects the morphology and sediment supply of the river.

Table of Contents

List of Figures

List of Tables

List of Appendices

Acknowledgements

This project required a good deal of physical labor, by many people, at the field study site, often under less than ideal conditions. I would like to thank all of those people, especially Rob Gieck, Heather Best, Paul Overduin, Matt Fraver, John Gallagher, and Greta McGee.

I'd also like to thank Andrew Balser, of UAF's Institute of Arctic Biology, for his assistance with collection and processing of the GPS data used in this study.

Finally, I'd like to thank Dr. Larry Hinzman, Dr. Douglas Kane, and Dr. Robert Carlson of the University of Alaska Fairbanks, and Dr. James McNamara of Boise State University, for their assistance and guidance throughout this project. Their help has been has been invaluable and is greatly appreciated.

Funding for this project was provided by the USGS State Water Institute Program and the NSF Office of Polar Programs, Arctic System Science Program (OPP-9814984).

1. Introduction

Arctic rivers differ from those of more moderate climates in that ice is present in the channels for eight or more months a year. Also, due to the continuous permafrost presence, there is little or no baseflow during these winter months and the headwaters and shallow reaches of these river channels freeze solidly to the riverbed. This condition is referred to as bottom ice.

In the Arctic, all precipitation from approximately October through May is stored as snow and then released over a 6-20 day snowmelt runoff period. This snowmelt runoff is often the major hydrologic event of the year, frequently of channel-forming competence. However, in the headwater and shallow reaches of these rivers, where most of the sediment in the river system would originate, the bottom ice armors the riverbed and banks, protecting them from sedimentation processes.

Evidence suggests that the morphology of arctic river systems is controlled by the presence of permafrost and river ice. McNamara et al (1999) have proposed that arctic river systems are underdeveloped as result of the effect of permafrost on hillslope processes. McNamara (2000) has also proposed that the armoring provided by bottom ice dominates the morphology of the portions of these rivers that experience bottom ice. Best (2002) presented evidence pertaining to hydraulic geometry and downstream grain size fining that supports this hypothesis.

The primary objective of this study is to investigate the potential amount of bedload transport that is not realized due to the presence of bottom ice in the Upper Kuparuk River.

Bottom ice affects bedload transport in three ways:

1) By armoring the bed material and preventing bedload transport during the competent snowmelt runoff flows.
2) By creating bedload movement through ice rafting of material (Figure 1.1). This occurs when material embedded in bottom ice is transported and deposited downstream when the ice breaks free from the bed during high snowmelt runoff.
3) By enhancing bedload movement in localized areas. This can occur when higher topographic areas, such as bar tops, of the riverbed become exposed through the bottom ice. When this happens, the local bed material is exposed to high velocities and flow turbulence due to the thin laminar sublayer that occurs upstream of the exposed area. In addition, these areas are also exposed to scour from ice blocks that are entrained in the flow.

Through three seasons of field observations on the Upper Kuparuk River, the dominant effect of the bottom ice is the suppression of bedload transport. Ice rafting certainly occurs; however, there were only 8-10 occurrences observed during this study. The bedload transport rate via this mode seems likely to be in the range of kilograms per hour rather than the kilograms per second rate that would occur in an ice-free channel.

Localized scour was also observed one time during this study. This mode seems to be a more likely source of appreciable bedload movement. But for this

situation to arise it appears that the initial channel ice thickness must be less than nominal. In 2001, the ice thickness was below average and the snowmelt runoff period was prolonged due to cold, cloudy weather. This led to a case were the runoff never exceeded the banks of the river and the flow very effectively

Figure 1.1 Ice rafting on the Upper Kuparuk River (June 2001).

eroded the ice. By the time the runoff discharge peaked there were some bar tops exposed and in one case there was bedload movement. Again though, the rate of transport, taken over space and time, is likely to be very low. To further reduce the importance of this mechanism, this condition likely occurs infrequently.

This study relied primarily on tracer rocks and channel cross-section surveys to monitor bedload movement. The study began in June of 2000 with the

installation of 201 tracer rocks ranging in size from 20mm to 200mm. In June 2001, an additional 200 tracers were installed, including 19 radio transmitter tracers with motion sensors. The radio tracers were intended to provide knowledge of incipient motion that could be used to identify the minimum competent discharge.

The ideal scenario for this study would have been to have comparable competent events occur during snowmelt and during the ice-free season. However this did not occur and the competent discharge threshold and bedload rating curves used in this analysis were calculated using established techniques.

During the summer of 2000, there were no events generating competent flows. The peak discharge during the snowmelt runoff of 2001 was comparable to the minimum calculated competent flow and there was some slight movement of 14 of the 201 tracers. This movement occurred on a bar top that was observed to be exposed through the bottom ice, and was attributed to localized scour, as described above. One tracer was rafted a significant distance downstream.

During the snowmelt runoff of 2002 there was an excessive amount of ice in the channel until well after the snowmelt runoff recession, and no tracer movement occurred. Through the summer of 2002, there were no competent flows until the storm of record for this site occurred the week of August 15th.

This event was caused by approximately 5 centimeters of rainfall, in an 18-hour period, on top of approximately 40 centimeters of wet snow. In addition to shutting down the Dalton highway, washing out culverts, and damaging Trans-Alaska Oil Pipeline service roads, this event generated a tremendous amount of bedload movement and morphologic response in the study reach. All tracers moved and most were buried and lost. The entire bed was mobilized, with the

exception of random boulders in the half-meter and above size classes. The flood peaked at a stage of 2.4 meters (approximately 98 m^3/s) and shortly after the hydrograph peak the gauge site was washed out.

There are two sections to this thesis. The first contains an analysis of the flow history of the Upper Kuparuk gauge site (1993-2002) to determine approximately how much bedload transport potential is not realized due to the bottom ice presence during the snowmelt runoff period.

The second section contains an analysis of the August 15th, 2002 event. The focus of this analysis is the estimation of bedload transport rates via tracer rock movement. This section also contains an investigation of the reach-scale morphological response to this event.

2. Background

2.1 Arctic Rivers

Arctic rivers are dominated by the presence of ice in all forms. During the long, cold winters a large percentage of arctic rivers freeze solid. Areas that maintain some amount of flow through the winter are covered with up to two meters of surface ice, or cap ice. Frazil ice, a term used to describe the small clumps of ice that form in supercooled waters and tend to stick to any surfaces they come into contact with, and anchor ice, which is a solid ice layer that forms on the bed material of the river channel, can form in arctic rivers throughout both the fall freeze-up and the snowmelt break-up periods. In many years, this leaves only two months when rivers of the Arctic are completely free of ice.

There is very little available in the literature regarding the effects of bottom ice on bedload transport or channel morphology. McNamara (2000) has conducted a study of the hydraulic geometry of the entire length of the Kuparuk River, in Northern Alaska. The focus of this study was the relationship between drainage area and hydraulic geometry. The results of this study indicate a discontinuity in the relationship between these variables that appears to be coincident with the extent of bottom ice for this river (Best, 2002).

Hodel (1986) introduces several characteristics of the Sagavanirktok River, including hydraulic geometry, sediment load, and hydrology, of the river that occupies the watershed directly east of the Kuparuk River. This paper is

intended to be an overview and the controls on these parameters are attributed to ice, permafrost, and climate without detailed consideration or discussion.

Another study of rivers in the Alaskan Arctic (Scott, 1978) investigates the effect of permafrost on channel behavior. This research focused on the timing and depth of thaw in several rivers of the region. Scott reported that in fine-grained channels the scour process was retarded by frozen bed material for as much as three weeks after the breakup period. He concluded that limited sediment availability, due to frozen ground and ice, in arctic rivers plays a role in reducing the total sediment load in these rivers.

A common thread among these studies is that the total sediment load in arctic rivers is low in comparison to rivers of more temperate climates (Syvitski, in review) and that ice and permafrost are the major factors in this condition. While this is the common conclusion among many studies of fluvial processes in the Arctic, few studies take the next step by attempting to quantify these effects.

Most of the published research into the relationship between river ice and sediment transport involves the interaction between frazil ice or anchor ice, and small particles, more so than with larger bed materials (Kempema et al., 1993). These studies focus on the process of frazil flocs forming, settling on the bed, and agglomerating fine materials that can then be lifted and transported by the buoyant forces of the frazil flocs. The formation of frazil ice and the potential for frazil flocs to transport fine sediment are of concern in many high latitude engineering applications such as hydropower and water supply intakes (Terada, et al., 1999).

Woo and Sauriol (1981) published a study of the effects of snow jams on fluvial activities in the Arctic. This study was performed near Resolute, in Canada’s

Northwest Territories, on the McMaster River and its tributaries. This study site varies significantly from the Kuparuk River in that parts of this study involved ephemeral channels which at the onset of snowmelt runoff were not continuously filled with ice, but rather were primarily covered with snowpack, and that below the snowpack, bed materials are exposed. They conclude that snowmelt competence is high, as observed by the entrainment of large boulders in exposed areas, but that large portions of the channel are protected by the snowpack and the magnitude of fluvial erosion is limited by the snowpack.

A study of the significance of sediment rafting was performed on the Albany River in Ontario, Canada (Martini et al., 1993). They report that the sediment load rafted accounts for less than 1% of the total annual sediment load and that, in the study location, the rafted material was primarily fine grain sizes. They further conclude that ice rafted material is insignificant, but that the depositional patterns of ice rafted material can be a useful tool in understanding geomorphologic and geologic processes.

There have also been studies of the effects of ice jams on channel morphology. One of these studies performed in Western Canada (Smith, 1979) related ice jams to unusually large return periods for a bankfull flow condition. This may, or may not, have implications on the hydraulic geometry of the lower reaches of the Kuparuk River; but in the headwater reaches, the channels freeze solid and ice jams have little, if any impact.

2.2 Incipient Motion

Bedload transport can be described as a random phenomenon that is generated by the interaction of turbulent flow structure with the materials of the bed surface (Einstein, 1950). This interaction is very complex, and as a result, attempts to model this process have largely resulted in limited or qualified success.

There have been two general approaches towards the concept of bedload transport. The first, and most popular approach is through the use of a critical variable such as shear stress, stream power, discharge, or velocity. This approach assumes that there is no bedload transport until the critical variable has been exceeded by the flow conditions, and that the bedload transport rate increases in proportion to the increase in the flow condition beyond the critical value.

There have been numerous studies, both in natural channels and in flumes, based on this concept and there are a large number of these transport rate equations in the literature. Use of these equations depends on the conditions under which the equations were developed.

The second approach, introduced by Hans Einstein in 1942 (Einstein, 1950), is based on a probabilistic approach to bedload movement. A motivation for this approach was the difficulty in establishing a critical criterion, as described above, and a belief that variables such as ‘step length’ and ‘rest period duration’ are best modeled as random variables. This approach offered new insight into bedload transport processes. However, the level of complexity made application of this method to natural channels very difficult (Yang, 1996).

Perhaps the most common approach for determining incipient motion of bed material is the critical shear stress method using Shields parameter based on the median particle size of the bed material population. The Shields diagram is based on dimensionless parameters and relates the particle Reynolds number to the critical shear stress through the dimensionless critical shear stress parameter, or Shields parameter. Shields diagram is shown in Figure 5.1.

The value of the Shields parameter has been shown to vary between approximately 0.03 and 0.08 (Buffington and Montgomery, 1997). Determination of the precise value of Shields parameter is very difficult in natural channels, and the choice of this value is critical in accurately determining incipient motion of bed material. Most all bedload transport equations that utilize an excess shear stress technique assume a Shields parameter value.

2.3 *Bedload Transport*

In gravel and cobble bed rivers, channel maintenance is related to bed material transport (Leopold, 1992; Emmett and Wolman, 2001). However, bedload transport measurements are difficult to make in large part because the flows necessary to generate movement also make direct measurements virtually impossible (Ryan and Troendle, 1997).

There are three techniques that are often used make bedload transport measurements. Each of these has advantages and disadvantages. The methods are:

1) Bedload samplers, such as the Helley-Smith bedload sampler, which capture material as it moves.
2) Bedload traps, which are typically fixed in a channel and also capture material in motion.
3) Bedload tracers, which are seeded in a channel, moved during a competent event, and then relocated to provide insight into the movement of individual or groups of particles.

The most common sampling method for measuring bedload transport is the Helley-Smith sampler. This device has been used to develop many data sets

(Emmett et al., 1996) and is particularly useful in channels that are very active at lower flow levels that permit wading.

When using the Helley-Smith sampler, measurements are made at intervals across a channel cross section and then the results are integrated to determine a total transport rate at that cross section. A weakness of this method is that even during competent flow periods, most bedload particles are stationary most of the time (Schmidt and Ergenzinger, 1992; Chacho et al., 1989). So the issue of sampling duration and frequency can be a factor in the accuracy of the results. Standard protocols for using these type samplers have been established in an effort to limit sampling errors.

This type of sampler is not particularly useful for the study that was performed on the Kuparuk River because of the remoteness of the area, the size of the channel, the size of the bed material, and the magnitude of the event required to generate bedload movement.

Bedload traps have also been used in a number of studies. These range from buckets buried in the river channel that collect moving particles as they fall into the bucket, to very elaborate mechanized systems.

The majority of the studies using bedload traps use simple pit-type designs, which are buried to the bed surface and emptied at regular intervals to estimate transport rates across the surface of the trap. The efficiency of these traps is a function of the trap opening size, and is considered to be very high for nonsuspendable particle sizes (Hassan and Church, 2001).

In addition to pit-type traps, vertically oriented traps have also been used to measure bedload transport.

The final method used to measure bedload movement is through the use of tracer particles. Tracers are particularly useful in course-grained rivers and in channels that experience bedload movement infrequently.

Tracers can be either active or passive. Active tracers are most commonly radio transmitters that can be implanted in particles and monitored via a radio receiver. Passive tracers are typically painted rocks. A metal or magnetic tag is sometimes added to the painted particles to facilitate recovering of buried particles through the use of a metal detector.

Tracer techniques are especially useful because they permit the total effect of a competent event to be observed through knowledge of the initial and final tracer positions, number of tracers moved, sizes of tracers moved, and final burial depth. None of these variables can be determined through the other two methods.

2.4 *Tracer Studies*

Because of the advantages described above, tracer techniques have become very popular for the study of bedload transport. Radio tracers have allowed valuable insight into the nature of bedload transport processes by providing information about movement frequency, distance, and rest periods of individual particles during competent flow periods (Schmidt and Ergenzinger, 1992, and Chacho et al., 1989). These tracers can also be equipped with motion sensors that can be used to provide incipient motion data, which is critical in determining the Shields parameter (McNamara, in review).

Passive tracers also offer many benefits with very little cost and complexity relative to radio tracer methods. Passive tracers allow the relationship between grain size, shear stress, and bedload transport to be studied (Ferguson and

Wathen, 1998), and offer insight into the concepts of size-selective transport versus equal mobility transport concepts.

Both Wilcock (1997) and Haschenburger and Church (1998) have presented methods for calculating bedload transport rates based on tracer particle movement. These methods are very similar and both of these techniques utilize the virtual velocity of the sediment to calculate a transport rate.

Virtual velocity is defined as the total average distance traveled for a population of particles during an event, divided by the total time of competent flow during the event. Typically the total time is estimated, as knowledge of incipient motion is rarely available in natural channel studies (Haschenburger and Church, 1998).

Several other variables that are difficult to measure directly are required for this calculation. These values include the active depth of the bed and the active width of the channel. While these are variables that in some cases cannot be measured directly, there are acceptable methods for estimating these values.

3. Study Site

The Kuparuk River is located in the northeast corner of Alaska (Figure 3.1). The channel initiates in the Brooks Range and flows north through the foothills, across the coastal plain, and to the Arctic Ocean. The total drainage area is 8140 square kilometers. The entire basin is underlain by permafrost, which ranges from 250 to 600 meters in depth (Osterkamp and Payne, 1981).

This study was performed in the upper reaches of the Kuparuk River, approximately 15 kilometers downstream from channel initialization, and just upstream from where the river intersects the Dalton Highway and the Trans-Alaskan Oil Pipeline. At this location the stream is 4^{th} order, based on USGS 1:63360 maps, and drains an area of approximately 146 square kilometers (McNamara et al., 1997).

The study focused on the river reach shown in Figure 3.2. The channel length through the study reach is approximately 400 meters. The channel has a meandering, alternate bar, pool-riffle morphology. The reach average slope is 0.0075. As Figure 3.2 shows, the study reach features one long, straight length of channel followed by a right hand bend and then a left hand bend.

The bed material is primarily cobbles with many boulders located throughout the reach. There is very little gravel in the thalweg of the channel, but significant amounts on bar tops. In Wolman pebble counts performed in the study reach, the D_{50} varied between 36 mm and 91 mm, depending on the location of the survey.

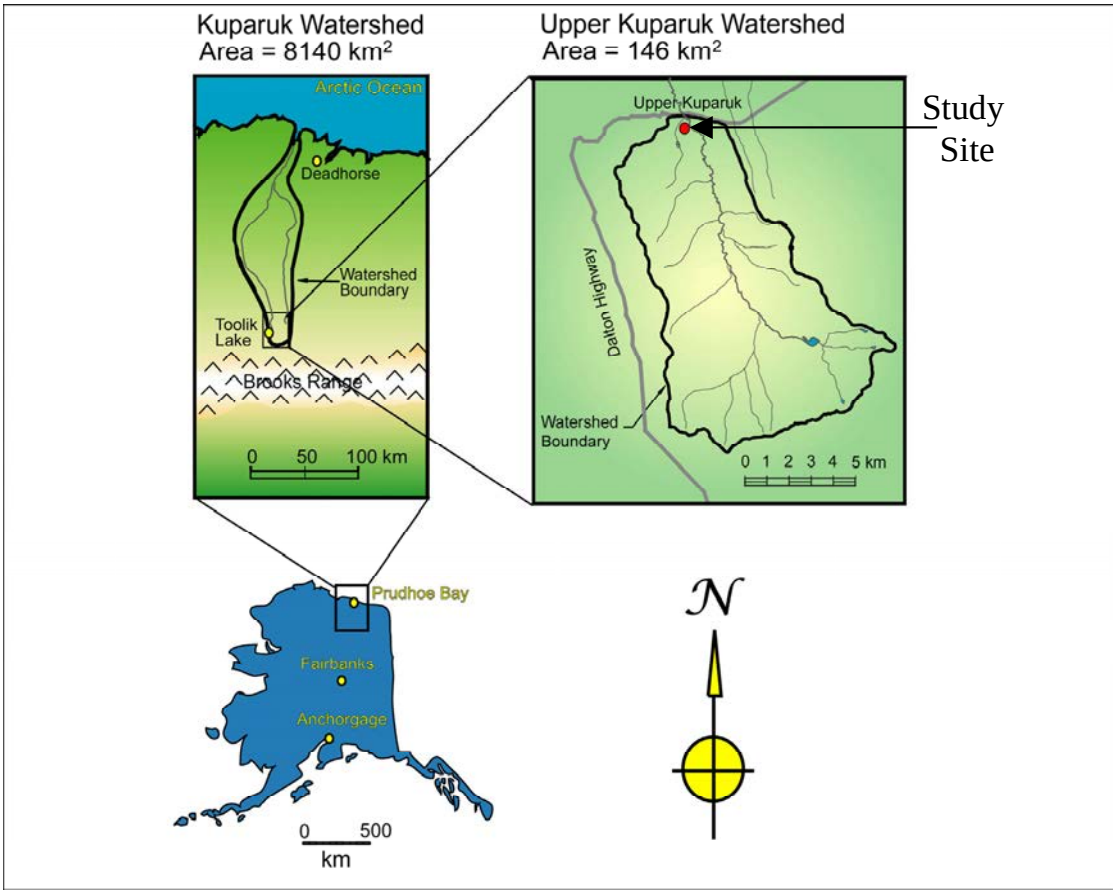

Figure 3.1 The Kuparuk River watershed with inset of the Upper Kuparuk River showing the study site location.

The study site is characterized by a broad alluvial floodplain with the primary vegetation being low shrubs and tussock tundra. Alternate banks tend to be steep with some amount of undercutting and sloughing occurring frequently. There is a distinct channel thalweg and the pool-riffle spacing varies from approximately one to five channel widths within the study reach.

The idealized river system is comprised of three zones. Zone 1 is the headwater area, which is considered the sediment production zone. Zone 2 represents the

transfer zone. And zone 3 is the depositional area. The location of the study site most closely matches zone 2 of the above river system description.

Using the Rosgen classification system, the study site is most closely matched to a C3 channel type (Rosgen, D., 1994).

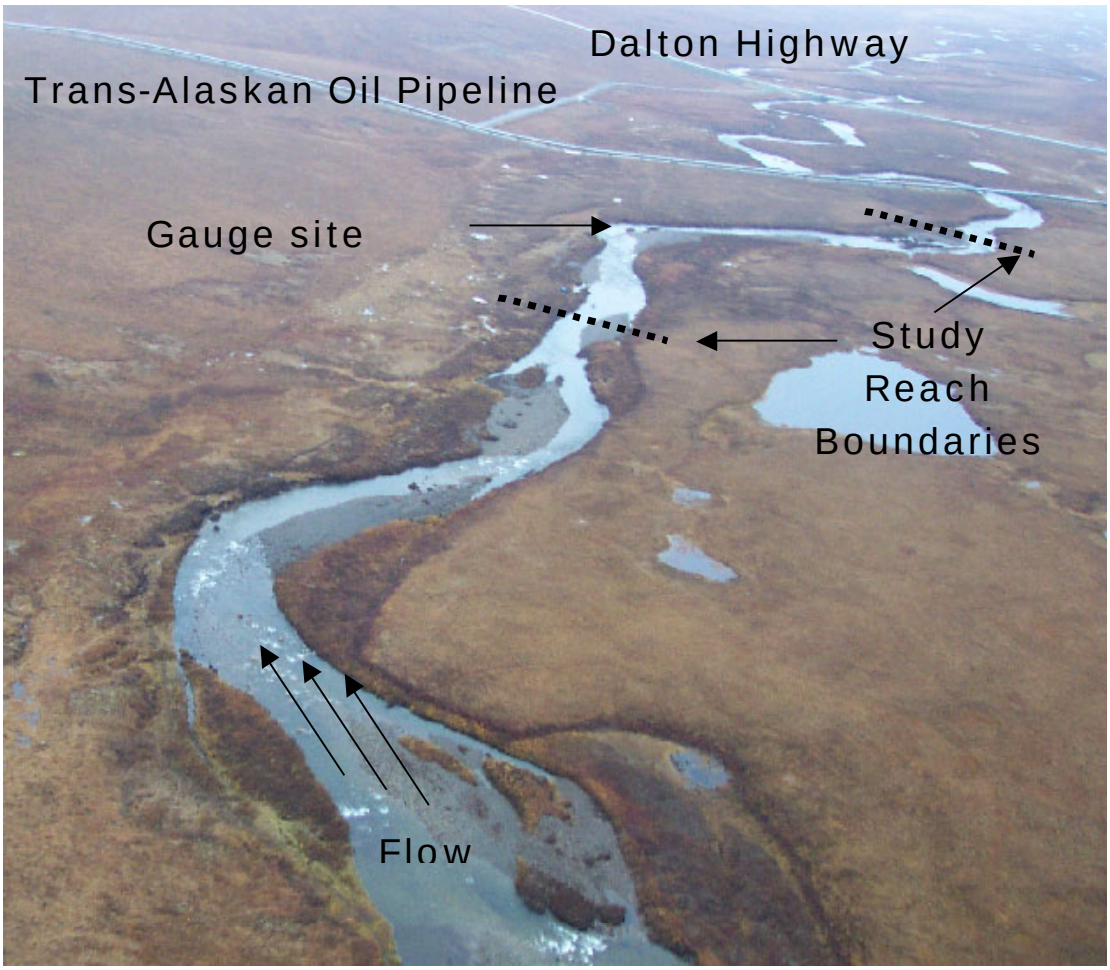

Figure 3.2 Aerial photograph of the Upper Kuparuk River study site (August 2002).

3.1 Hydrology

The hydrology of the region is dominated by the cold arctic climate. The open water season comprises only about four months of the year. Winters are long and once freeze-up occurs, typically in late September, all precipitation is stored as snow until the long daylight hours of May bring about the snowmelt period.

Through the summer months, precipitation occurs primarily as rainfall, although summer snowfall accumulations are fairly common. As Figure 3.3 illustrates, the snowmelt-generated discharge has been the largest annual event in four of the ten years that the site has been gauged. However, the largest discharge values, by far, have been due to the summer rainfall events of 1999 and 2002. All ten annual hydrographs are included in Appendix I.

A more detailed discussion on the hydrology of the Kuparuk watershed can be found in Kane et al. (1999).

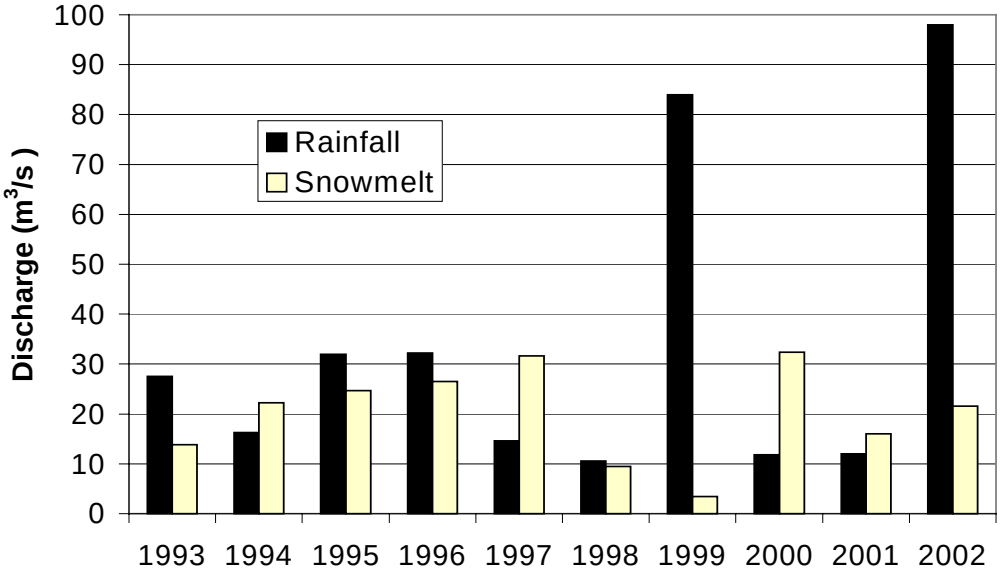

Figure 3.3 Annual maximum snowmelt and rainfall flood rates.

4. Field Methods

The remote location of the study site, combined with the infrequent nature of bedload transport in the Kuparuk River, made it impractical to monitor bedload transport continuously. Rather, the approach taken was to utilize methods that would allow the transport characteristics and morphologic responses to be intermittently measured, such as before and after major events. These methods included passive and active tracer techniques, bedload traps, cross sectional surveys, and Wolman pebble counts.

A photograph of the study reach is shown in Figure 3.2 and a planform map of the study site is shown in Figure 4.1. This figure shows the five cross sections that are the focus of this study. Cross sections 1,3, and 4 are permanent cross sections that are part of a long-term morphological monitoring project. Cross sections 1+ and 2 are the initial locations of the tracer rocks.

4.1 Passive Tracers

Two groups of passive tracers, in the form of brightly painted rocks, with epoxy coating to protect the paint, were used. The first group of 201 orange painted tracers was installed in June of 2000. This group ranged in size from 30 mm to 270 mm, and was placed at cross section 2 in Figure 4.1. These tracers were placed on the bed surface with no effort to incorporate them into bed material. This location is at the top of a long, steep riffle.

A second group of passive tracers was added in June of 2001. This group of 182 yellow painted tracers was located slightly downstream from cross section 1, near the lower end of a deep pool. Again, these tracers were placed on the bed surface. The tracers ranged in size from 30 mm to 230 mm with a median size of 85 mm. Because these tracers are located in the same pool as cross section 1, throughout this study the yellow tracers are considered to be located at cross section 1. A photograph showing both of the tracer rock cross sections is shown in Figure 4.2.

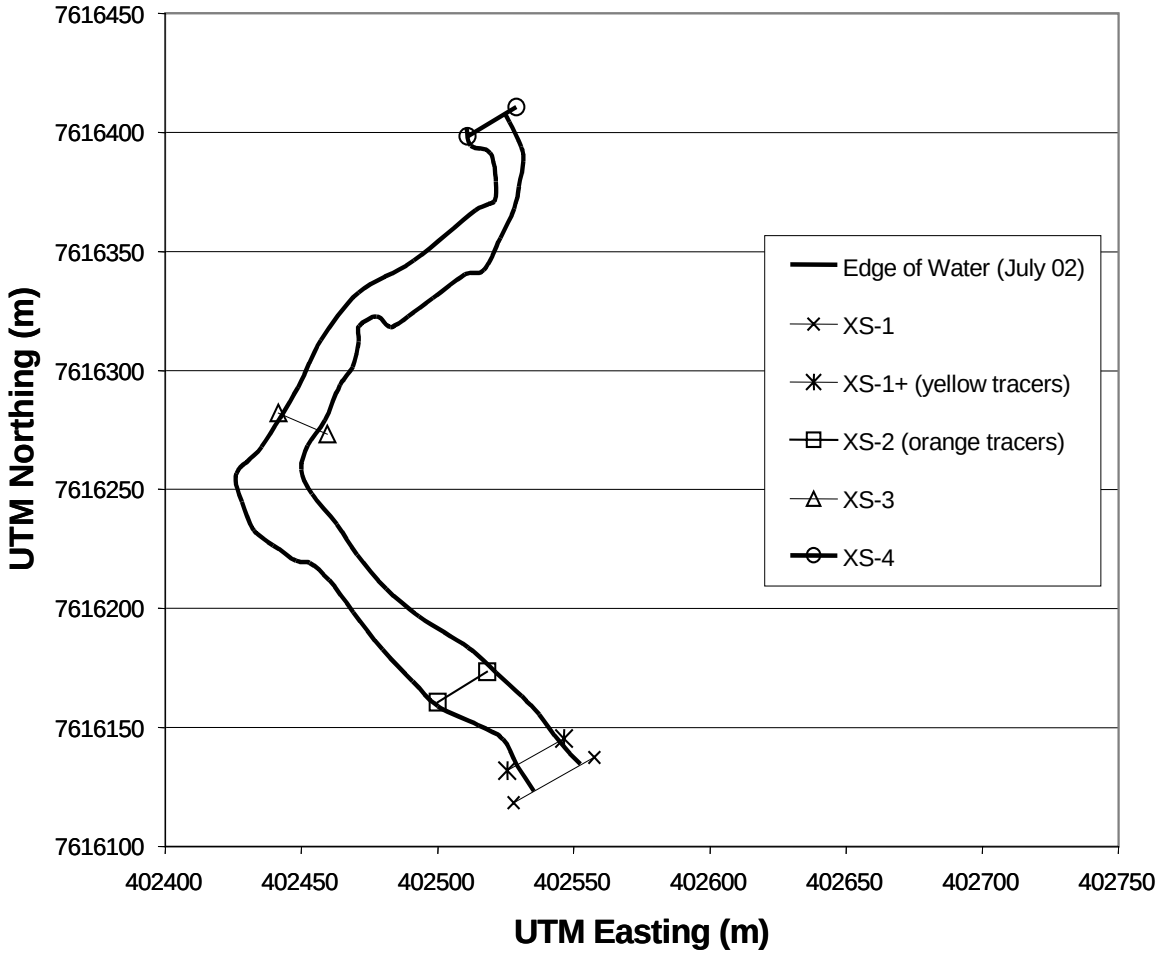

Figure 4.1 Planform map of the study site showing the five cross sections that are the focus of the study.

4.2 Active Tracers

A group of 19 radio transmitter tracers were added to the orange tracer cross section in July of 2001. These tracers ranged in size from 50 mm to 150 mm. The transmitter and three of the tracers with the transmitters installed, can be seen in Figure 4.3.

The radio transmitters were programmed to emit two different signals. One signal indicated that the rock was stationary. A second signal indicated that the rock was in motion. The motion signal was intended to provide knowledge of the onset of movement, which could be used to determine the critical shear stress value at the time of incipient motion.

A Telonics radio receiver and signal processor was used to monitor the radio transmitter signals, and a Campbell Scientific CR10X data logger was used to record all signals.

The transmitters had a useful battery life of approximately 12 months and were intended to last from July 2001 through July 2002. This lifespan was achieved by using a quiescent standby period through the winter months from October 1st, 2001 through May 1st 2002.

4.3 Survey Data

This study relied heavily on survey data to monitor changes in channel cross-section due to bedload movement. Cross sections 1,3, and 4 have been surveyed twice a year since 1999. These cross sections are surveyed as soon as the snowmelt runoff recession begins and again at the end of the open water season in late August or early September, to identify any changes that may have occurred during the snowmelt runoff or as a result of summer rainfall events. In addition to cross sectional surveys, detailed topographic surveys were performed

in July of 2002 and again in September of 2002. The majority of the survey data were obtained using a total station electronic theodolite. Some survey data were also obtained using a Trimble survey grade GPS unit.

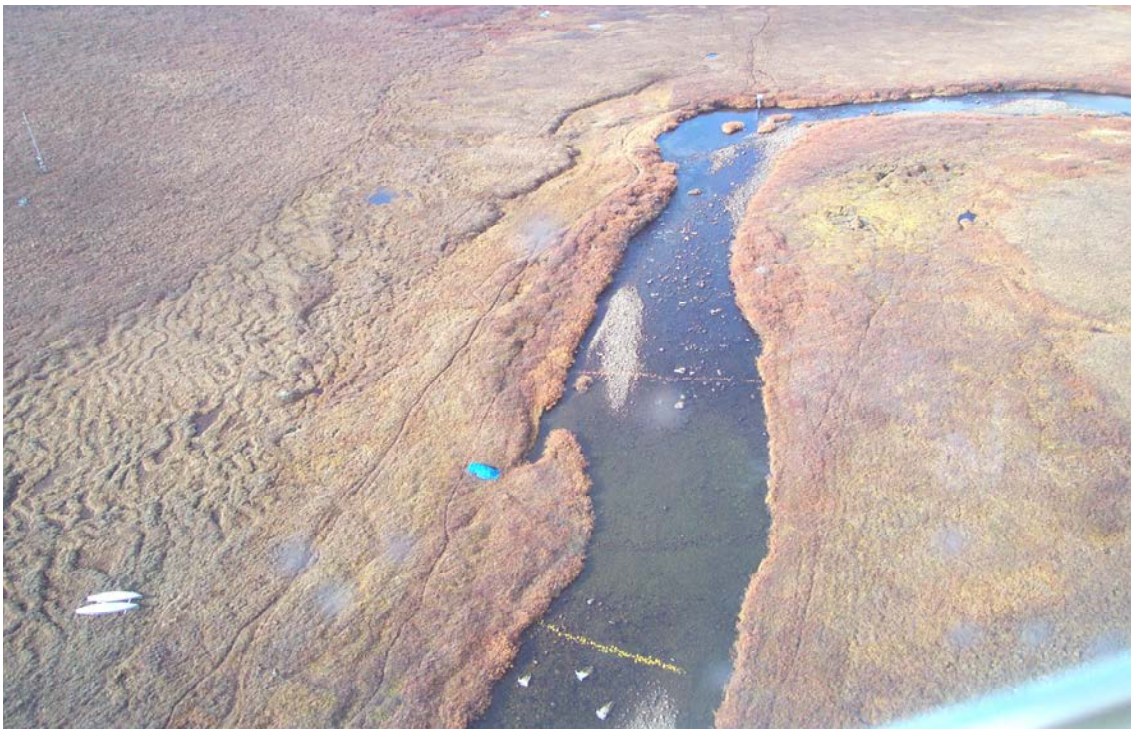

Figure 4.2 Tracer rock cross sections (September 2001).

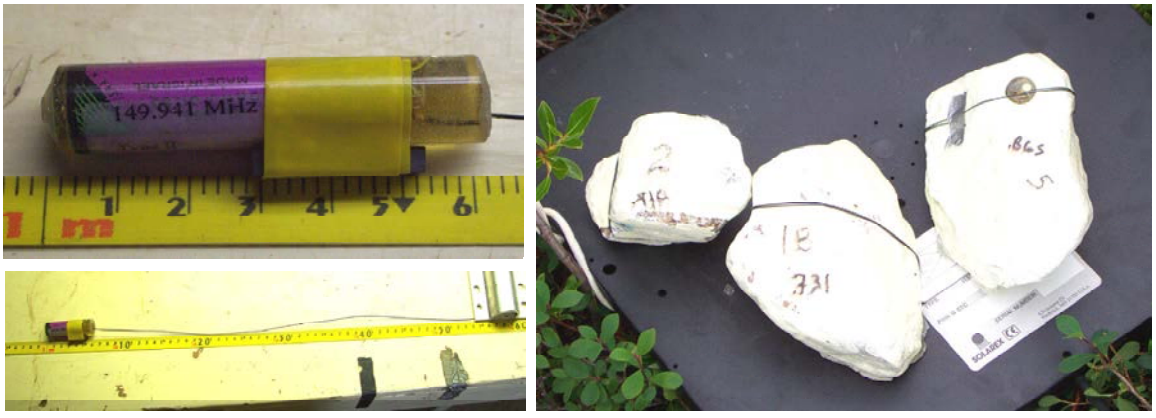

Figure 4.3 Radio transmitter used in active tracers (left top and bottom) and three active tracers prior to deployment (right) (July 2001).

4.4 Bedload Traps

Vertically oriented bedload traps were used in an attempt to capture bedload material while in motion (Figure 4.4). These traps have been used successfully in smaller mountain streams where they were installed and removed during high flow events (Bunte, 2001). The Kuparuk River does not offer this opportunity. These traps were placed in the channel and checked approximately every two weeks. This technique did not work well as organic matter quickly clogged the nets (Appendix II) and prevented any bed material from entering the traps.

4.5 Scour Chains

Scour chains are chains that are driven into the bed material and used to monitor scour and deposition. After an event, buried chains can be located with a metal detector and the material covering the chain can provide information about the size of material that was moved during the event. If scour has occurred during an event there will be more links exposed than there were prior to the event.

4.6 Bed Material Grain Size

Wolman pebble counts were performed at eight different locations within the study reach to determine the surface material size distribution. In addition to surface material distributions, subsurface grain size surveys were determined on the bar in cross section 1, both before and after the August 15th, 2002 event.

In determining the subsurface grain size distribution (Figure 4.5), an area of 1m x 1m was randomly selected. A surface pebble count was then performed. After that, the bed material was removed to a depth of approximately $2D_{84}$ (approximately 17 cm in this case). A volume of approximately 40 liters of material was then removed from the area and sorted by size class. The size classes were then weighed and counted down to the 4 mm size class. Plots of all cumulative grain size distribution data are included in Appendix III.

Figure 4.4 Bedload trap as installed in the Upper Kuparuk River (August 2001).

Figure 4.5 Subsurface pebble count. The area outlined (top left), surface pebble count performed (top right), material removed from area (bottom left), subsurface material sorted by size class (bottom right). (July 2002).

Part I:
Bedload Transport Potential During Snowmelt Runoff

5. Analysis Methods

The objective of this analysis is to determine how much potential bedload transport is suppressed due to the presence of bottom ice during the competent flows of the snowmelt runoff period for the Upper Kuparuk River. The procedure for doing this requires four steps:

1) Establishing a threshold discharge value that defines the incipient motion of the median particle size for the river reach at cross sections 1, 2, 3, and 4 (Figure 4.1).
2) Using the flow history for the study site, determine how often and for how long the threshold discharge is exceeded.
3) Using established relationships, determine the bedload rating curve for each cross section.
4) Using the bedload rating curves of part 3) and the competent flows of part 2), determine how much bedload transport is suppressed due to the presence of bottom ice.

5.1 Incipient Motion Calculations

Bedload movement occurs as a result of lift and drag forces exerted on the particles. Shear stress is often used as a proxy for these forces. In this study, a dimensionless critical shear stress, or Shields parameter, approach was used to determine the discharge threshold for incipient motion. The relationship is given by the following equation:

$$\tau^*_c = \tau_c / g\,(\rho_s - \rho)\,D_{50} \qquad 5.1$$

Where,

τ^*_c = dimensionless critical shear stress, or Shields parameter
τ_c = shear stress at incipient motion
ρ_s = sediment density
ρ = fluid density
D_{50} = median particle diameter
g = gravitational constant

The Shields diagram is shown in Figure 5.1. Using an experimentally determined, or assumed value for the Shields parameter, the shear stress at incipient motion can be calculated as:

$$\tau_c = \tau^*_c\, g(\rho_s - \rho)\,D_{50} \qquad 5.2$$

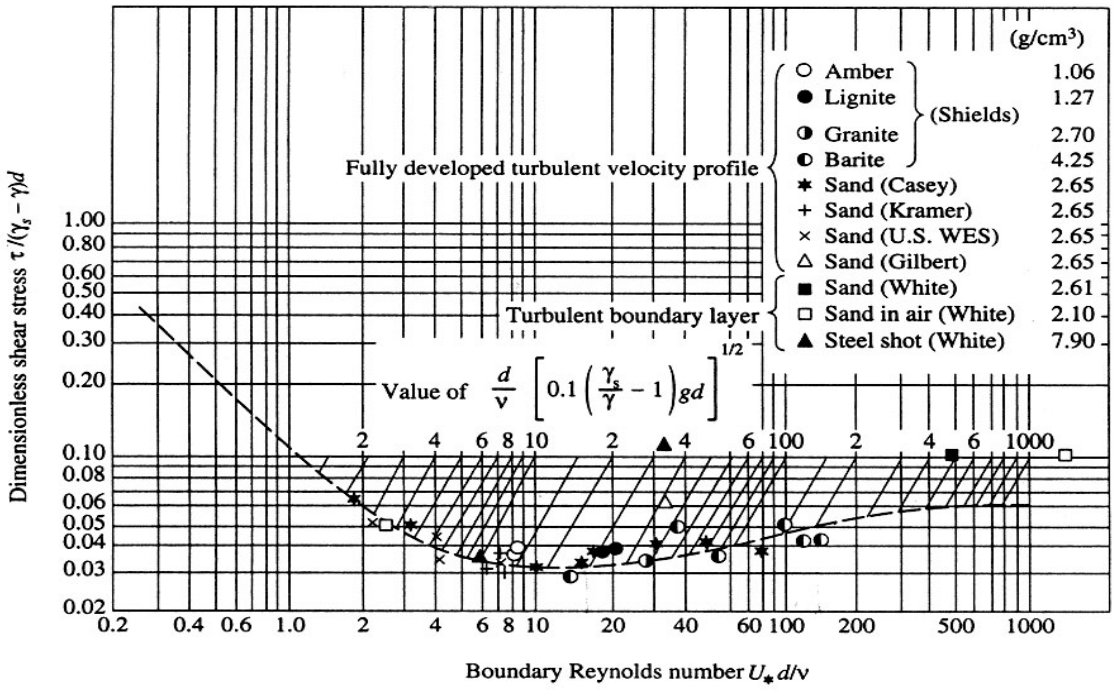

Figure 5.1. The Shields diagram for incipient motion (Yang 1996).

Once the critical shear stress is calculated the hydraulic radius can be determined using the following relationship:

$$\tau_c = \gamma RS \qquad 5.3$$

Using the surveyed channel cross sections, the discharge required to obtain the critical shear stress can be determined. This value is the threshold, or minimum competent flow.

5.2 Competent Flow Periods

Hourly flow data for the Upper Kuparuk gauge site is available from May 1993, through August of 2002. These ten years of flow data were used for this analysis. The hydrographs for each year are included in Appendix I.

These data sets begin with the onset of snowmelt runoff and extend to near the end of the open water season, accounting for 28,056 hours of discharge data. The complete data set covers1169 days of open water over ten seasons. The data were sorted by the hourly discharge value, from maximum to minimum. The competent flows were then separated and those due to snowmelt runoff were identified.

5.3 Bedload Rating Curves

Two methods were used to generate bedload rating curves at cross-sections 1, 2, 3, and 4. The methods chosen were the Meyer-Peter and Mueller equation (1948) (Yang 1996), and Parker's (1990) equation. These methods were chosen partly because they tend to give different results, especially for high excess shear stress conditions. They were also both based on, and have proven to work well with, data obtained from gravel bed rivers of moderate gradients.

The Meyer-Peter and Mueller equation is:

$$\gamma(K_s/K_r)^{3/2} RS = 0.047(\gamma_s - \gamma)d + 0.25\rho^{1/3}q_b^{2/3} \quad 5.4$$

Where,

γ, γ_s = specific weights of water and sediment (metric tons/m^3)
R = hydraulic radius (m)
S = energy slope
d = mean particle diameter (m)
ρ = density of water (metric tons/m^3)
q_b = bedload transport rate (metric tons/s/m^3)
K_s = Strickler's coefficient
K_r = Coefficient of particle roughness

The Parker (1990) method utilizes a two-phase relationship between a dimensionless bedload transport parameter (W^*) given by:

$$W^* = \begin{cases} 0.00218 \exp [14.2 (\varphi_{50} - 1) - 9.28(\varphi_{50} - 1)^2] & \text{for } 1 < \varphi_{50} < 1.59 \quad 5.5 \\ 11.93 (1 - 0.853/ \varphi_{50})^{4.5} & \text{for } \varphi_{50} > 1.59 \quad 5.6 \end{cases}$$

and a dimensionless shear stress parameter based on the median grain size that is given by:

$$\varphi_{50} = \frac{DS}{0.0875 (\gamma_s/\gamma - 1)d_{50}} \quad 5.7$$

This relationship was developed for the Oak Creek, Oregon field data set shown in Figure 5.2. This data set illustrates the variability inherent to bedload transport rates.

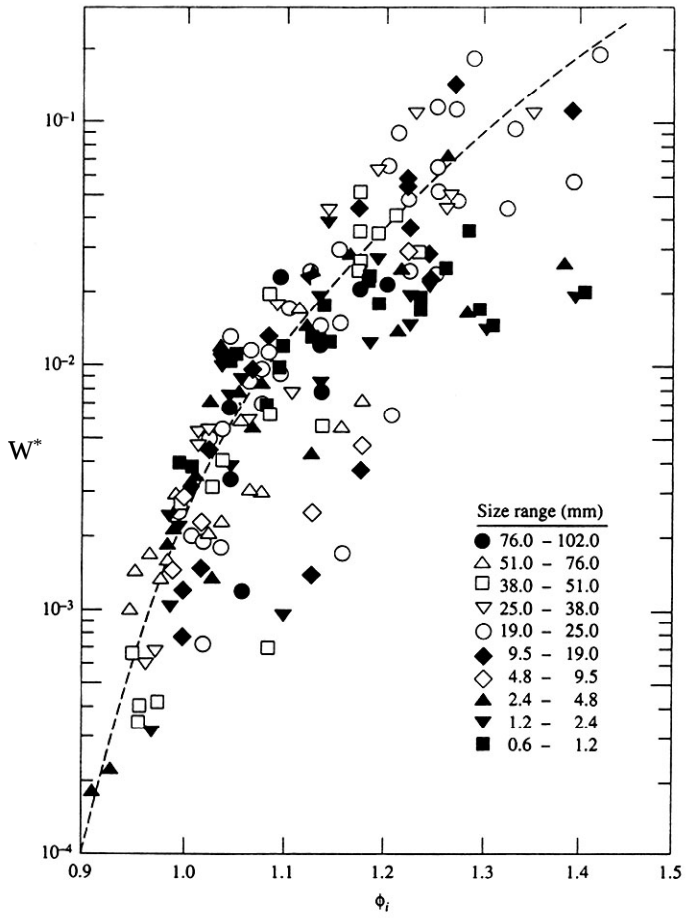

Figure 5.2 Plot of W^* vs. φ_{50} for the Oak Creek, Oregon data with indicated size ranges (Yang 1996).

The relationship between the dimensionless bedload transport function, W^* and bedload transport, q_b is given by the following equation

$$W^* = \frac{(\gamma_s/\gamma - 1)\, q_b}{(gDS)^{1/2}\, DS} \qquad 5.8$$

In the above equations;

D = flow depth, m

S = energy slope

γ_s, γ = sediment and fluid densities, kg/m^3

d_{50} = median particle size, m

q_b = bedload transport rate, kg/s/m

g = gravitational constant

5.4 Potential Bedload Transport

The potential bedload transport was then calculated by applying the bedload rating curves developed in section 5.3 to each hour of competent flow that occurred during snowmelt runoff between 1993 and 2002, as identified in section 5.2. This analysis was performed at cross sections 1, 2, 3 and 4.

This analysis assumes that the net bedload transport attributed to ice rafting and localized scour, as described in chapter 1, is negligible compared to the potential that could occur in an ice-free channel.

6. Results

The ideal situation for determining the effect of bottom ice on bedload transport would have been to compare the movement of the tracer rocks during a competent rainfall event in the summer and then observing the lack of tracer movement during an equivalent snowmelt period. Under this scenario, the radio transmitter tracers would have accurately identified the minimum ice-free competent discharge. However, during the useful life of the radio transmitters (July 2001 through July 2002) there were no competent ice-free flows, and therefore the radio transmitters did not provide any incipient motion data.

During the summers of 2000 and 2001, the maximum discharge was approximately 12 m^3/s and there was no apparent bedload movement. During the summer of 2002, the maximum discharge was the storm of record in August with a peak discharge value of approximately 98 m^3/s (See Appendix IV). This storm mobilized the entire bed and will be discussed in detail in the following chapter. The maximum snowmelt discharge values during this study were 16 m^3/s and 21.6 m^3/s in 2001 and 2002 respectively.

In 2001, there was initially very little ice in the channel, which led to the tops of some bars being exposed during the peak flows and there was some small amount of tracer movement. During the 2002 snowmelt, there was a great deal of aufeis in the channel and much of the floodplain. The ice persisted well beyond the snowmelt runoff period and, despite the competent discharge, there was no tracer movement.

6.1 Minimum Competent Discharge

Since no ice-free competent flows occurred, with the exception of the extreme event of August 2002, the minimum competent discharge was calculated rather than determined via field data. In order to calculate a competent discharge value using the method of 4.2.1, the Shield's parameter had to be estimated and the median particle size had to be determined.

To determine the median particle size, Wolman pebble counts were performed ten times at the eight locations shown in Figure 6.1. The median particle size ranged from 36 mm to 91 mm with the reach-average median size being 57 mm.

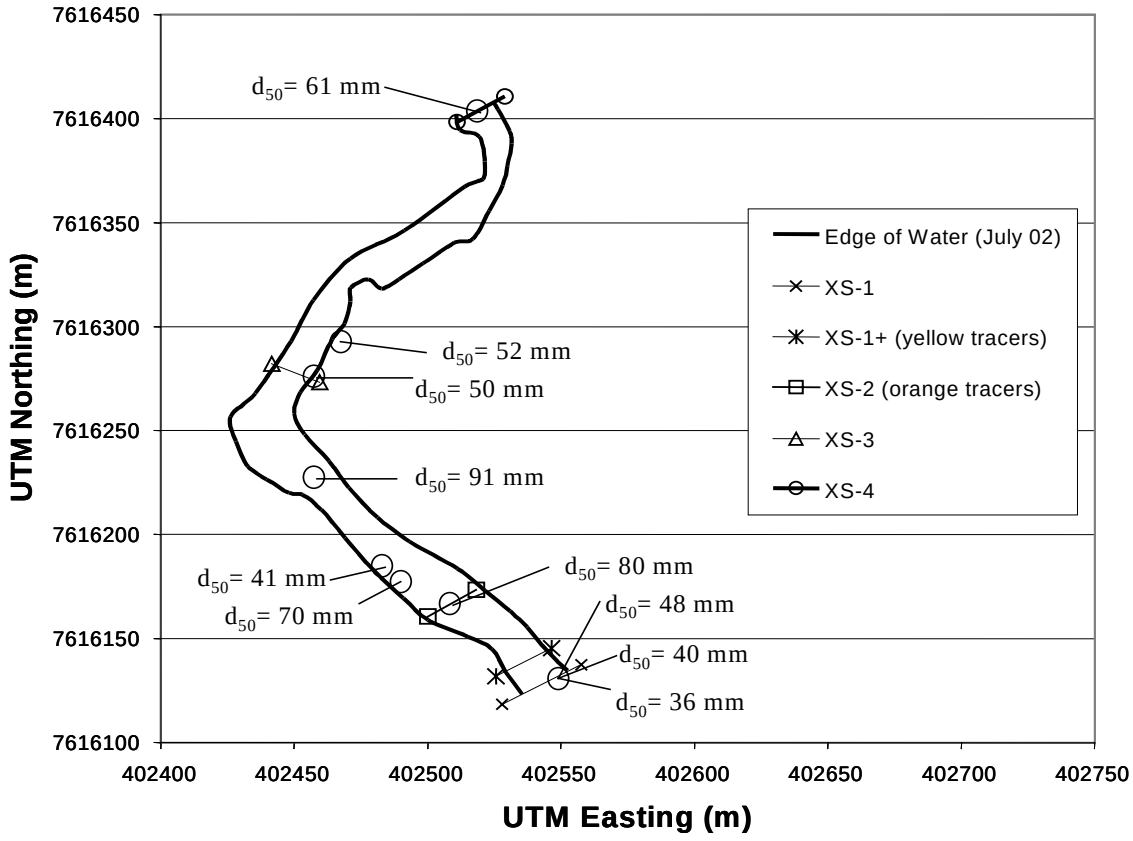

Figure 6.1 Locations of surface pebble counts with median grain size. All data was obtained between June 2000 and September 2002.

Due to the channel depth most of the grain size data was obtained on gravel bars or in shallow sections of the river. However, the channel thalweg contains mostly larger material that was not completely accounted for by the survey locations shown in Figure 6.1. For that reason, the reach average value was assumed to be a slightly larger value of 70 mm.

The Shield's parameter is difficult to determine in natural channels. If a competent discharge had occurred while the radio transmitters had been functional this value could have been calculated. Based on the peak flow value that did not result in tracer rock movement, the Shields parameter was determined to be greater than 0.032.

With no further information, the approach taken was to make the common assumption that incipient motion occurs at high boundary Reynolds numbers. Under these conditions, the Shields parameter is approximately 0.06 by Figure 5.1. This value is conservative, and is not likely to result in an overestimate of the amount of competent flow that has occurred during snowmelt. Using this value and a median particle size of 70 mm, the critical shear stress was calculated to be 68 N/m^2 using Equation 5.2.

Using the survey data for cross sections 1, 2, 3, and 4, which are included in Appendix V, and the relationship of Equation 5.3, the respective minimum discharge required to generate 68 N/m^2 was calculated to be 14.4, 19.2, 15.1, and 16.6 m^3/s.

In proceeding with the analysis, the minimum competent discharge was taken to be 15 m^3/s. All flow levels less than the threshold value were ignored as not capable of generating bedload transport and ignored. All values greater than this value that occurred during the snowmelt runoff period were evaluated for their

transport potential according to the Meyer-Peter and Mueller and Parker's methods of section 5.3.

6.2 Competent Flow Periods

The hourly flow history (1993-2002) for the study site was analyzed to determine how often the minimum competent flow occurred and what percentage of those times occurred during snowmelt runoff when the bed was armored by bottom ice.

This analysis showed that during the open water season, the threshold flow value was exceeded for only 694 of 28,056 hours (2.47%) of data (Figure 6.2). Also, of these 694 hours of competent flow, 428 hours (61.7%) occurred during the snowmelt runoff period when the probability of generating bedload movement is very low due to the bottom ice presence. Another 124 hours (17.9%) of competent flow occurred during the two large individual events of July 1999 and August 2002.

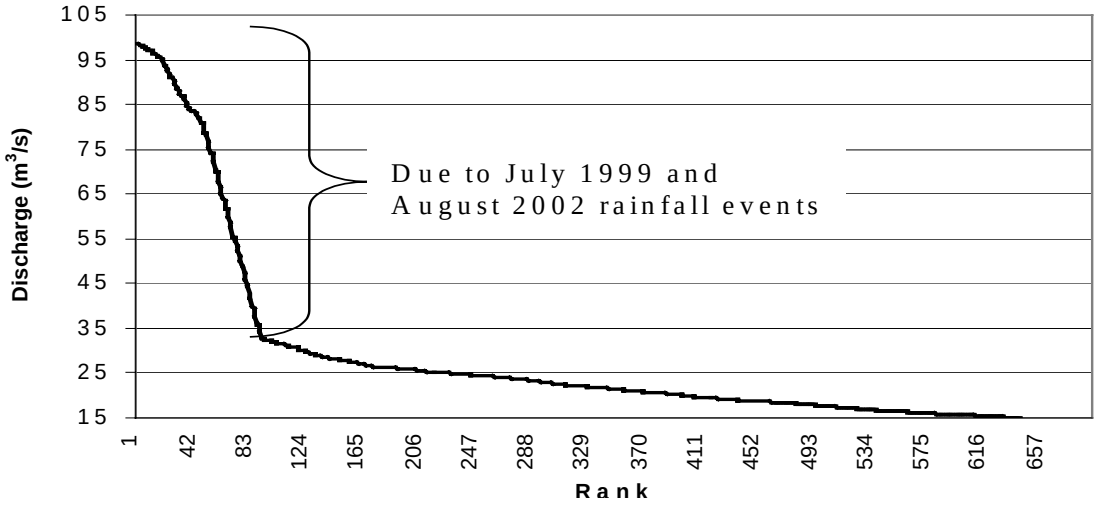

Figure 6.2 Rank of competent hourly flow values for the Upper Kuparuk River between 1993 and 2002.

6.3 Bedload Rating Curves

The following four figures show the Meyer-Peter and Mueller, and Parker (1990) bedload rating curves, as well as the discharge rating curve for each of the four cross sections.

Among these four figures, only the bedload rating curves for cross section 4 predict any bedload transport at discharge values as low as the 15 m^3/s value that was calculated in the previous section. As would be expected, the three cross sections located in pools (1,3, and 4) all have significantly lower thresholds for bedload transport than that calculated for the riffle of cross section 2. This is due to the broader, shallower channel geometry of the riffle cross section.

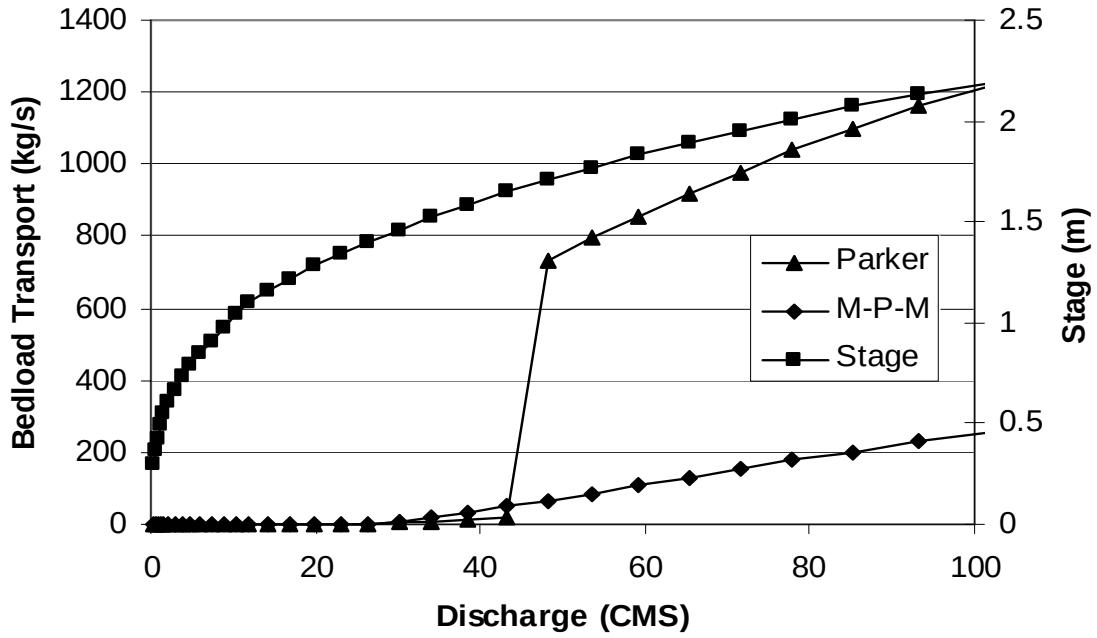

Figure 6.3 Rating curves for cross section 1.

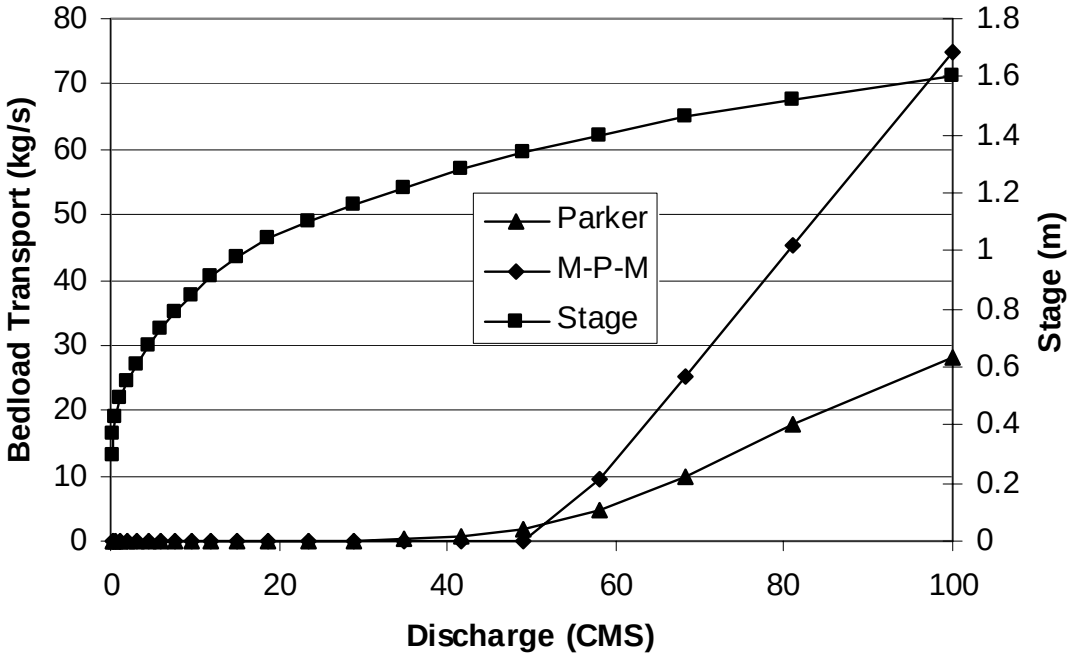

Figure 6.4 Rating curves for cross section 2.

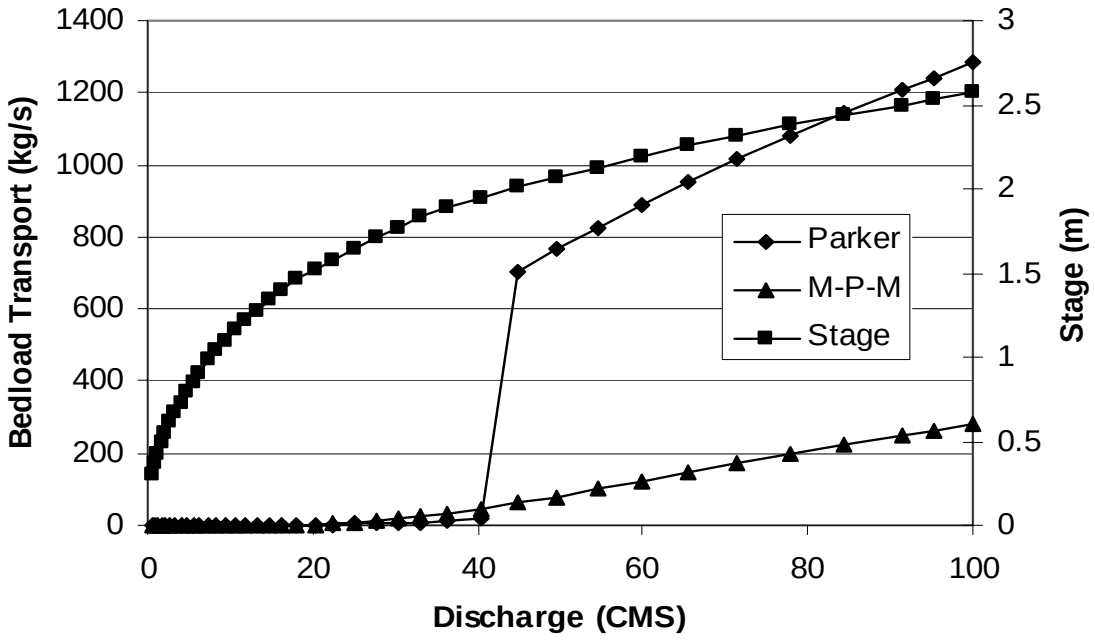

Figure 6.5 Rating curves for cross section 3.

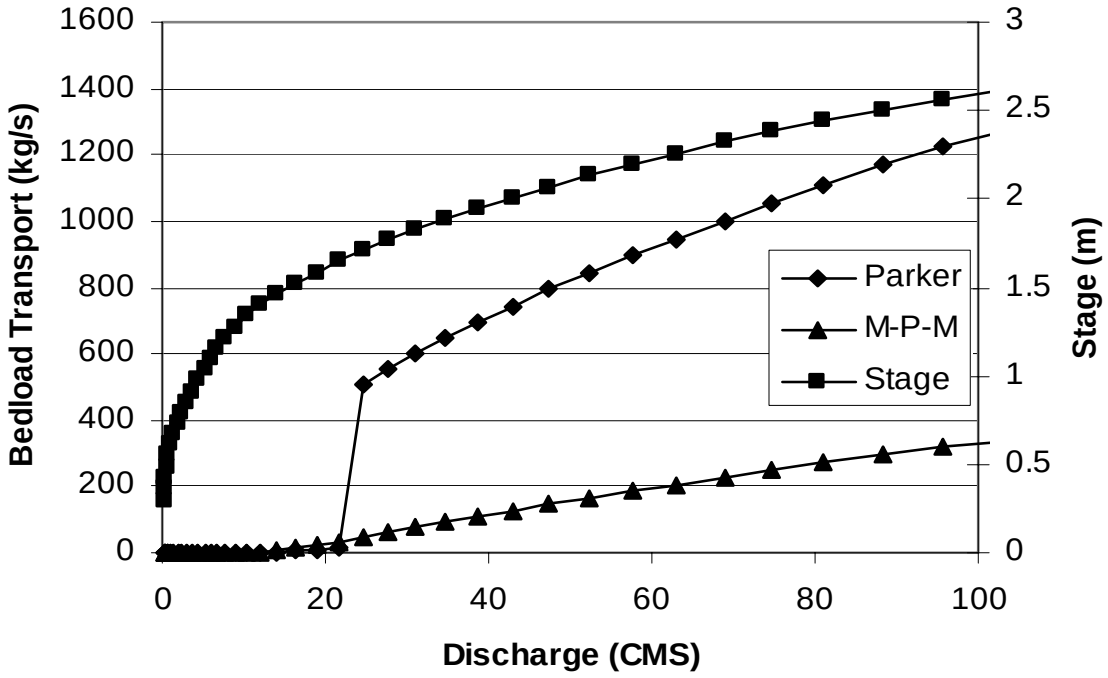

Figure 6.6 Rating curves for cross section 4.

6.4 Potential bedload transport

The potential bedload transport refers only to transport that is not realized due to the presence of bottom ice. The potential bedload transport was determined by applying the bedload rating curves of section 6.3 with the portions of Figure 6.2 that occurred during the snowmelt runoff period. The results, by yearly total, for each cross section are shown in Figures 6.7 through 6.10. The total potential lost bedload transport between 1993 and 2002, for each of the four cross sections, is shown in Figure 6.11.

These figures show that appreciable bedload transport potential existed for three of the ten years that were analyzed (1996, 1997, 2000), and that for the other seven years there was very limited potential, or no potential at all. Scour chain and survey data, obtained after the 2000 snowmelt runoff, support the hypothesis that no appreciable bedload transport occurred during this competent event.

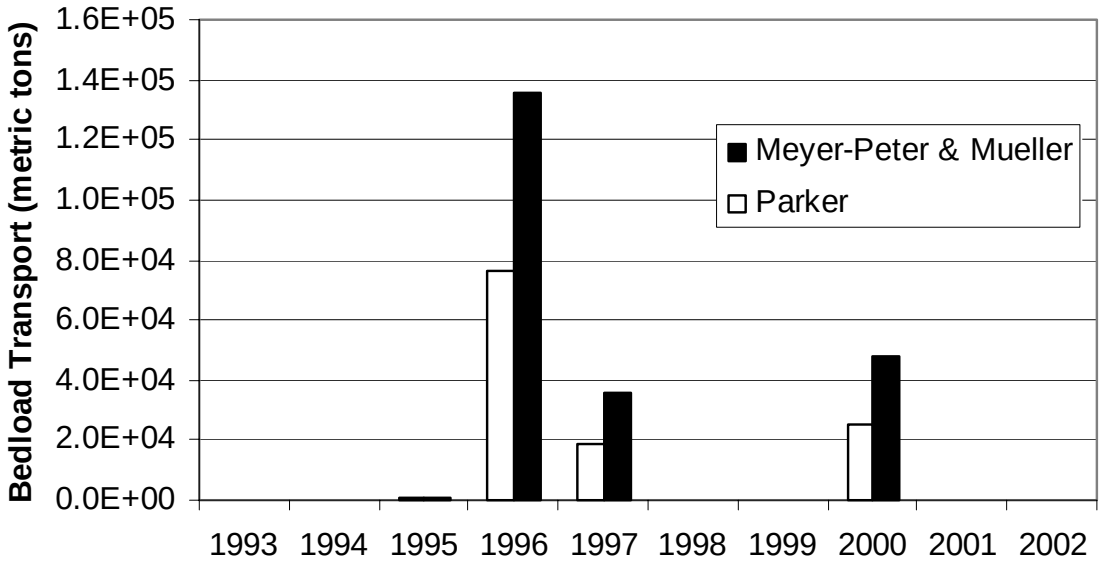

Figure 6.7 Potential bedload transport for cross section 1.

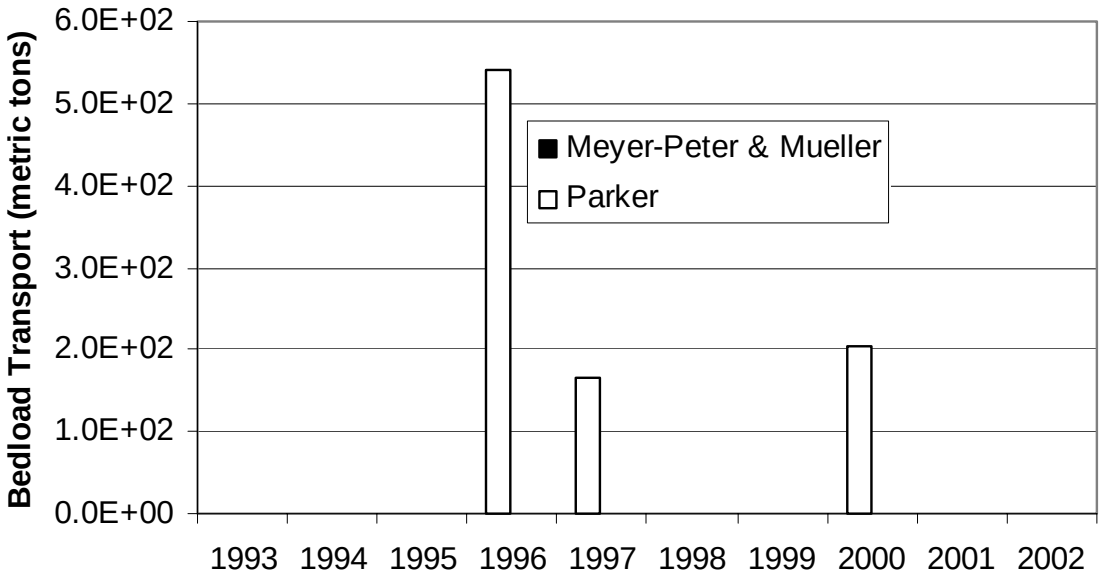

Figure 6.8 Potential bedload transport for cross section 2.

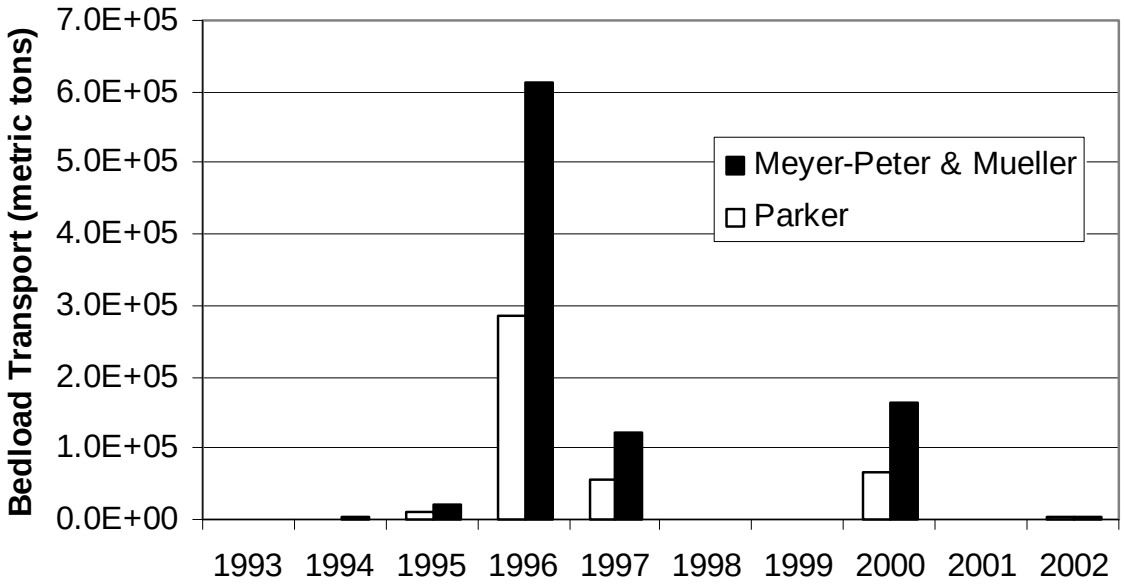

Figure 6.9 Potential bedload transport for cross section 3.

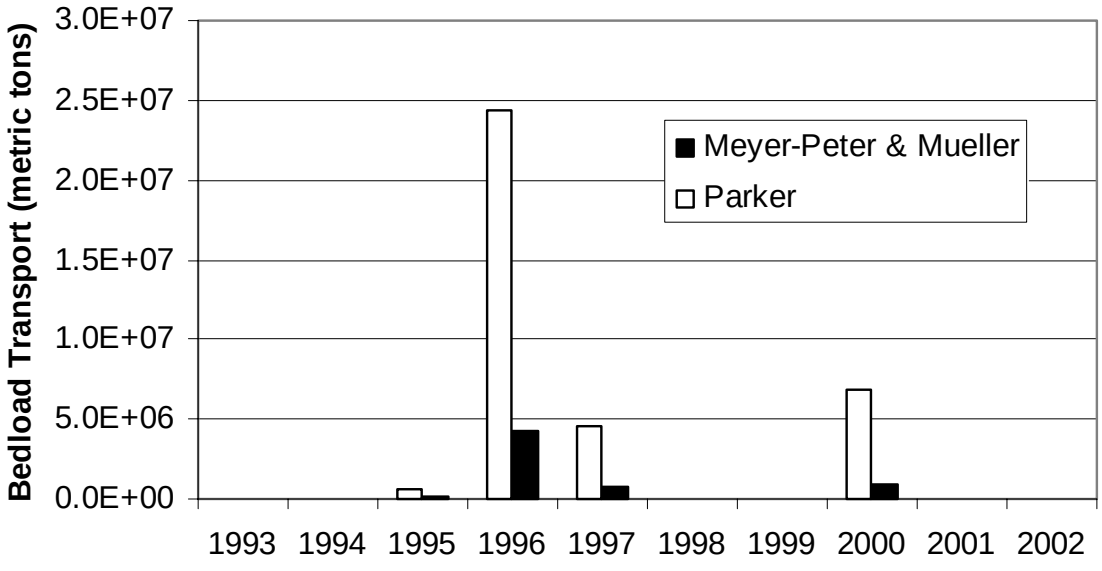

Figure 6.10 Potential bedload transport for cross section 4.

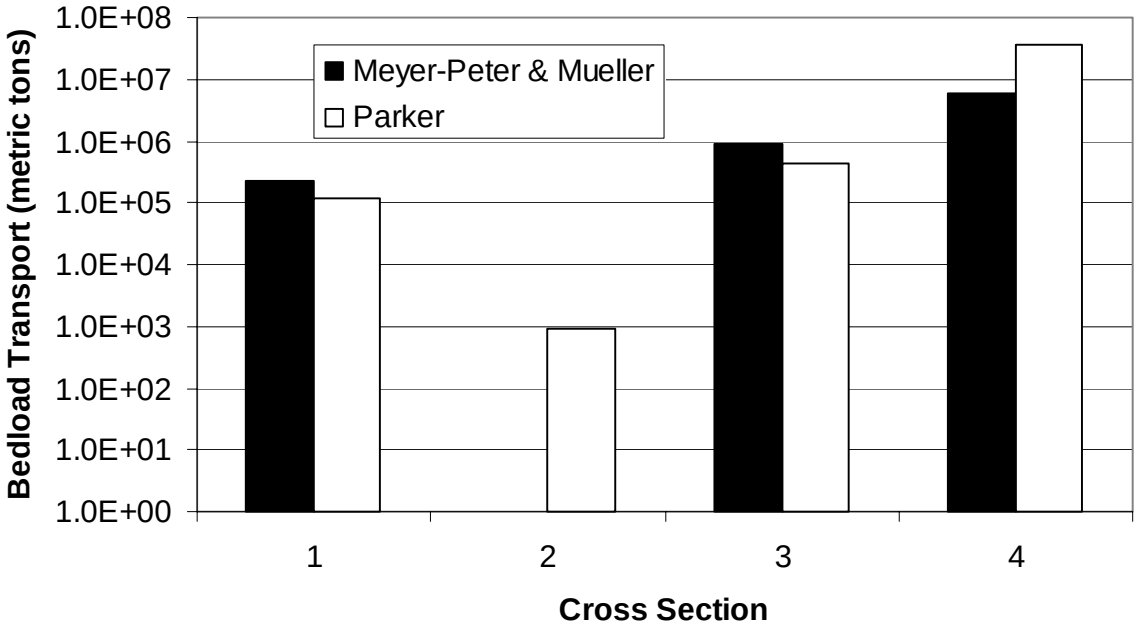

Figure 6.11 Total bedload transport potential by cross section for 1993-2002 (Note: Y-axis is logarithmic scale).

Figure 6.11 shows that for the three cross sections located in pools (1, 3, and 4) there is a significant amount of bedload transport potential over the ten-year data set. The values for cross sections 1, 3, and 4 average approximately one million metric tons of material transport that is not realized. Assuming a material density of 2650 kg/m^3 and a porosity of 0.25, this is equivalent to approximately 500,000 m^3 of material.

The analysis of cross section 2 predicts far less potential for bedload transport than the other three sections. Although to some extent this is possible, and it has been observed that bedload transport rates through pools are higher than those through riffles (Schmidt and Ergenzinger, 1992), the two are morphologically linked and it is clearly not possible to have three orders of

magnitude more transport through a pool than through an adjacent riffle. This variation in the predicted transport potential is an artifact of the inability to account for morphological controls using a cross-section based analysis. Its reasonable to expect that over this time period the channel would adjust to achieve a balance between the different cross sections.

An attempt was made to evaluate the affect of the lost bedload transport potential on the dominant, or channel forming, discharge for the study site. The dominant discharge occurs at the maximum value of the product of the flow frequency plot multiplied by the bedload rating curve (Knighton, 1998). This was done for two cases: one including the competent flows of the snowmelt runoff period, the other with those flows removed from the data set, which is the equivalent of assuming that no bedload transport occurs due to the bottom ice presence.

The 10-year data set is too short to draw conclusive results from the analysis. For this data set, the dominant discharge is equal to the maximum flow that had occurred during the period (i.e., the 98 m^3/s value of the August 2002 event) for both cases.

Part II:
Bedload Transport Rate and Geomorphic Response to a Major Hydrologic Event

7. Analysis Methods

The objective of this analysis is to use information obtained from tracer rock movement during the August 15th, 2002 event to estimate the average bedload transport rate, and also to use survey data and photographic information to study the geomorphic response of the channel to an event of this magnitude.

In addition, the bedload rating curves of Chapter 6 will be used to calculate an average bedload transport rate that can be compared to the value obtained using tracer rock data. This comparison provides an opportunity to validate the predictions of Chapter 6 and better understand the morphologic effects of the presence of bottom ice during the snowmelt runoff period.

7.1 Bedload Transport Rate

The bedload transport rate can be estimated as a function of the virtual velocity of tracer particles. The virtual velocity, v_b, is defined as the total distance traveled by individual tracer particles divided by the time interval over which movement occurred.

The approach used in this analysis was presented by Haschenburger and Church (1998), and Wilcock (1997). The relationship used to calculate the mass rate of bedload transport, G_b, is given by:

$$G_b = v_b\, d_s\, w_s\, (1\text{-}p)\, \rho_s \qquad 7.1$$

Where

v_b = virtual velocity of bedload material (m/hr)

d_s = the active depth of the streambed (m)

w_s = the active width of the streambed (m)

p = porosity of channel sediment

ρ_s = sediment density (kg/m^3)

G_b = mass transport rate of bed material (kg/hr)

This method represents an estimate of the average bedload transport rate as the first three terms of the equation can each vary temporally and spatially for a given flood event. Haschenburger and Church (1998) relate this transport rate to the stream power at the peak discharge value for the event. With the stream power calculated by:

$$\Omega = \gamma\, Q_p\, S \qquad 7.2$$

Where,

Ω = stream power per unit length of channel (W/m)

γ = specific weight of water (N/m^3)

Q_p = peak discharge (m^3/s)

S = channel slope

They also show a correlation between the stream power function and the calculated bedload transport rate for a study performed on Carnation Creek, in Western Canada.

The virtual velocity of the bedload material can be calculated directly from knowledge of the tracer material initial and final positions, and knowledge of the time interval between the initial and final movements. Typically this time interval

is taken as the total time that the minimum competent flow was exceeded during the event, as incipient motion data is rarely available in natural channel studies.

The active depth of the channel is the depth to which bed material is being mobilized. This is also a difficult parameter to determine, as there is generally no way to measure this directly during a flood event. There are however, several useful pieces of data that can be used to approximate this value, such as post-event channel cross-section surveys showing the depth of scour, burial depth of recovered tracers, and scour chains located in the river to monitor scour and deposition.

The active width is the width of the channel that contributes mobilized material. In marginally competent floods this can be less than the width of the channel. For a flood of the magnitude of the August 15, 2002 Kuparuk River event the active width can reasonably be considered to be the average channel width.

No direct measurements of bed porosity, p, were made for the Upper Kuparuk River, and there is very little data of this nature available in the literature. Leopold et al. (1964) presents an average value of 0.25 for gravel bed-rivers. This value was used in this analysis.

7.2 Sediment Supply

Dietrich et al. (1989) has proposed a dimensionless transport capacity, q^*, as an indication of sediment supply. The relationship for q^* is given by:

$$q^* = \left(\frac{\tau - \tau_{c50s}}{\tau - \tau_{c50ss}} \right)^{1.5} \qquad 7.3$$

Where,

τ = bankfull depth-slope product as given by equation 5.3

$\tau_{c50s,ss}$ = critical shear stress of the surface and subsurface material

A q^* value of 0 indicates a very low sediment supply. A value of 1 indicates a very high sediment supply.

8. Results

8.1 *Tracer Movement*

During the event of August 15th the entire bed was mobilized and all 402 tracers moved from their initial positions. A differential GPS unit was used to record the positions of all recovered tracers. The results of this survey are shown in Figure 8.1. An accounting of the recovered tracers is given in Table 8.1.

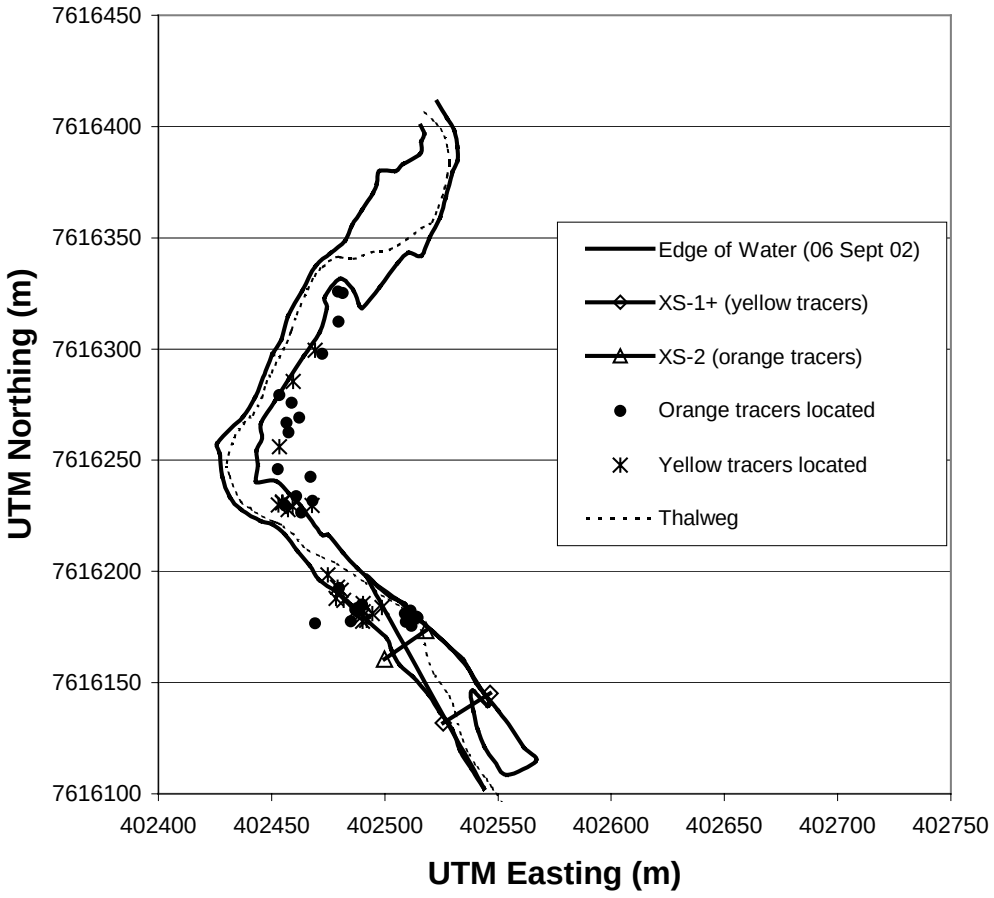

Figure 8.1 Map of tracer locations after the event of August 15th, 2002.

Table 8.1 Summary of the recovered tracer rocks.

Group	Initial Count	Recovered	%
Yellow	182	22	12.1
Orange	201	27	13.4
Radio	19	5	26.3
Total	402	54	13.4

The 13.4% recovery rate is low, even for visual tracers. Reports in the literature are frequently near 50% with many as high as 90% and 100% for small events (Church and Hassan, 1994, and Ferguson and Wathen, 1998). This can likely be attributed to the magnitude of the event, and the size of the channel. The bulk of the tracer rock studies in the literature have been performed in smaller channels with much smaller competent discharge levels. The 2002 event generated a great deal of topographic change in the bed with several areas aggraded by more than a meter, others that were degraded as much, and an appreciable amount of bank erosion. This will be discussed in more detail in the following sections.

The battery life of the radio tracers was intended to last through July of 2002. By August, only five transmitters were emitting any signal and none were transmitting motion signals, due to a lack of battery power. Four of these tracers were located and recovered. A fifth was located but not recovered, and was likely buried by as much as a meter of material under a bar that was formed during the event. Of the four recovered one was buried 30 cm deep, one was 15 cm deep, and two were imbricated in the surface layer. A yellow tracer was also recovered from a depth of approximately 30 cm while searching for a radio tracer.

A plot of the distance traveled for each particle is shown in Figure 8.2. This figure shows a trend of the decreasing maximum travel distance with increasing particle size.

The mean travel distance for all recovered particles was 72.8 m. The local morphology of the initial tracer placement appears to be a significant factor in the travel distance. The average travel distance for the orange and white tracers, which were placed at the top of a riffle in cross section 2, was 60.9 m. The yellow tracers, placed initially in the pool at cross section 1, traveled an average of 48% further at 90.1 m. This observation is consistent with the results of other tracer studies where pools are often reported to be more active than riffles (Schmidt and Ergenzinger, 1992).

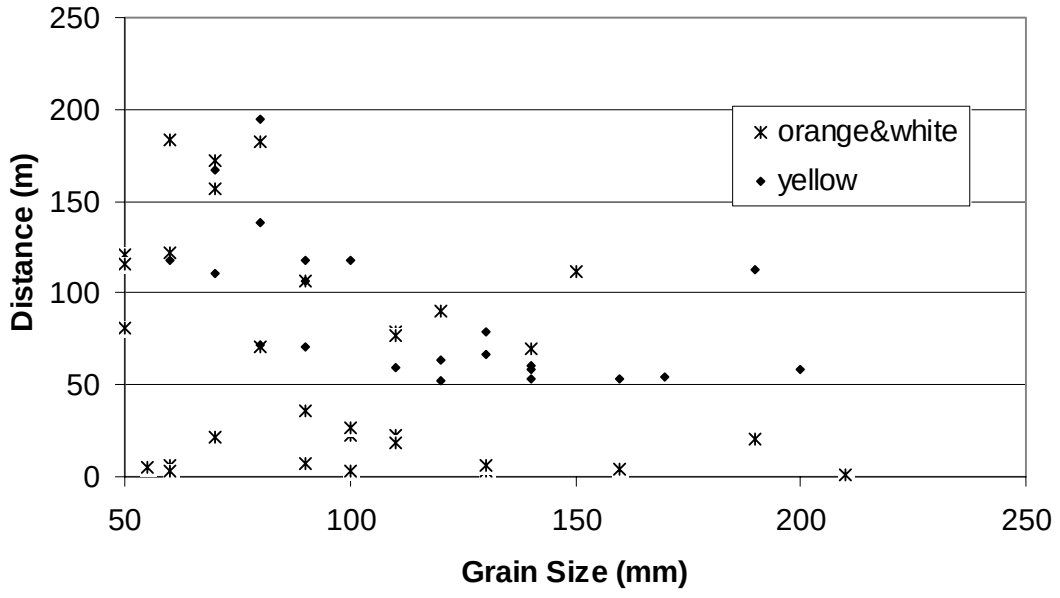

Figure 8.2 Travel distance for each of the 54 tracers recovered after the August 15th, 2002 event.

Figure 8.3 shows the average travel distances broken down by half-phi size classes. This is a classification system used frequently in geomorphology. In this system, the size class is given by 2^{ϕ}, with ϕ equal to; 5.5, 6.0, 6.5, 7.0, and 7.5. This figure does not indicate a strong correlation between particle size and distance traveled. This suggests that there was equal mobility among the all size classes during this event, which is often reported to be the case in course particle river channels, particularly when the entire bed is mobilized.

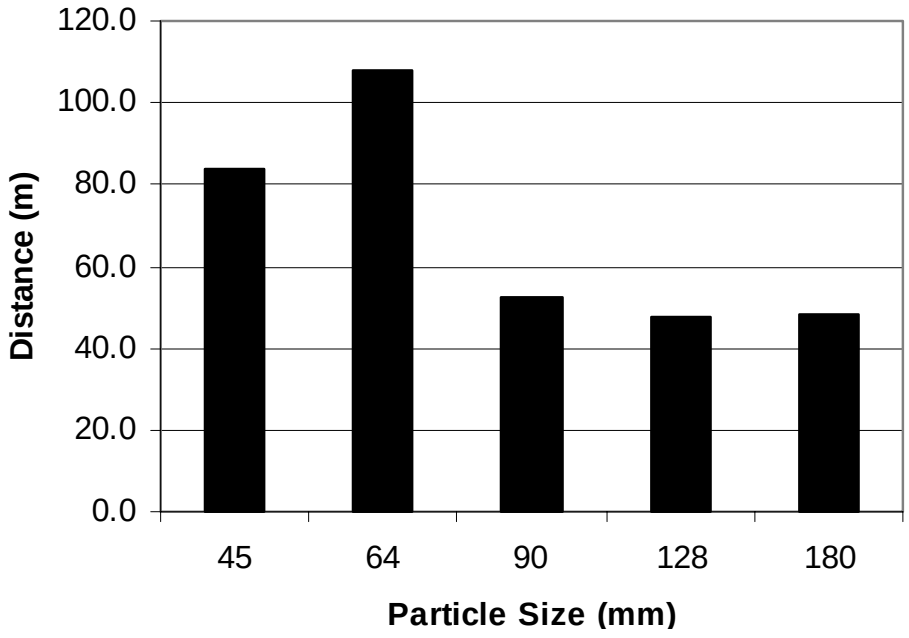

Figure 8.3 Average distance traveled for each half-phi size class recovered.

8.2 Bedload Transport Rate

The average travel distance was 72.8 m for all recovered particles. The time of competent flow is the amount of time that the flow exceeded 15 m^3/s. This value had to be estimated because the gauge recorder was washed out several hours after the hydrograph peak of the event. Therefore, the recession portion of the curve was estimated using the hydrograph from an 84 m^3/s event that occurred

in July of 1999. The estimated hydrograph is shown in Figure 8.4. This figure shows the competent flow period during this event to be approximately 53 hours. This results in a virtual transport velocity of 1.37 m/hr.

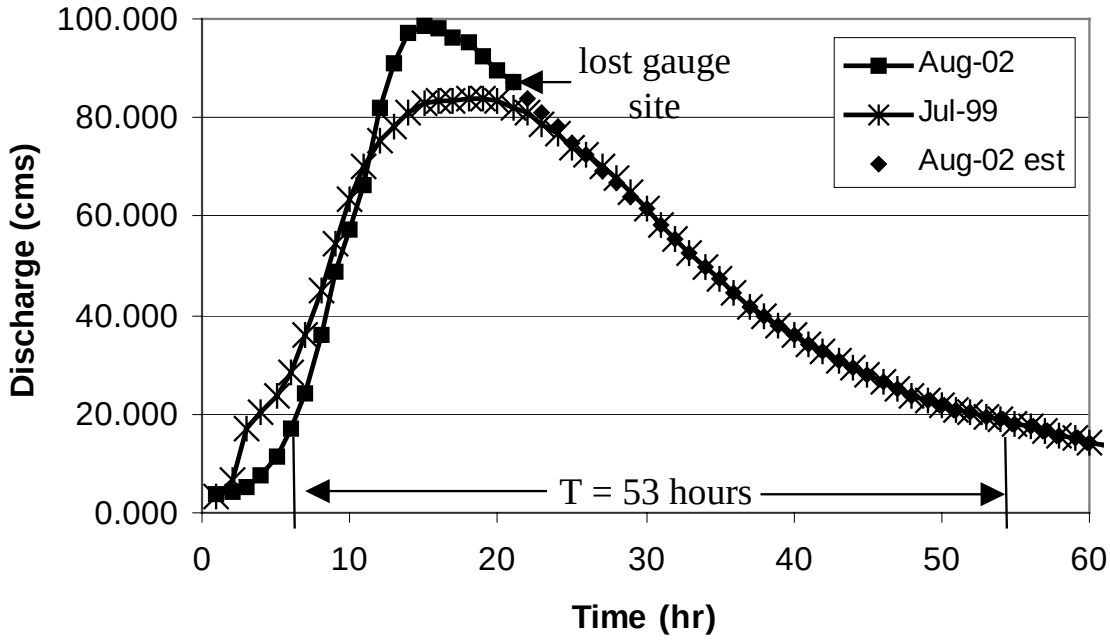

Figure 8.4 Hydrograph for the August 2002 event with the recession estimate.

The active depth was estimated to be 0.5m. This is assumed to be the average active depth across the channel width. This value is based on several pieces of data including surveyed erosion and depositional values, depth of recovered radio tracers, and the fact that several scour chains in the reach were no longer detectable using a metal detector that has a range of approximately 0.5 m.

The active channel width was assumed to be the average channel width, which is approximately 24 m based on several surveyed cross sections in the vicinity of the tracer rocks.

Using these values the average mass rate of bedload transport for the 53-hour event was calculated to be 32,700 kg/hr (9.1 kg/s), or, assuming a density of 2650 kg/m^3 and a porosity of 0.25, a volumetric rate of approximately 16.4 m^3/hr. By this calculation the event transported approximately 1732 metric tons (870 m^3) of material.

The maximum stream power for this event is 9500 W/m. When this value is plotted with the data presented by Haschenburger and Church (1998) for a similar study on Carnation Creek in British Columbia, Canada, the predicted transport rate appears to be slightly, but perhaps not significantly less than what was observed in that study.

The transport rate of 32,700 kg/hr (16.4 m^3/hr) estimated using the virtual velocity of the tracers compares fairly well to the amounts calculated using the bedload rating curves of Section 6.3 for cross section 2 (riffle). Using these rating curves, the average mass transport rate for this event is predicted to be 121,000 kg/hr (60.8 m^3/hr) using the Meyer-Peter and Mueller equation, and 59,400 kg/hr (29.9 m^3/hr) using the Parker equation.

8.3 *Morphologic Response*

A significant morphological response was generated by this event. The primary changes involved the modification of existing bars, creation of new bars, and severe bank erosion. The changes to the study reach were well documented by survey and photographic data obtained before and after the event.

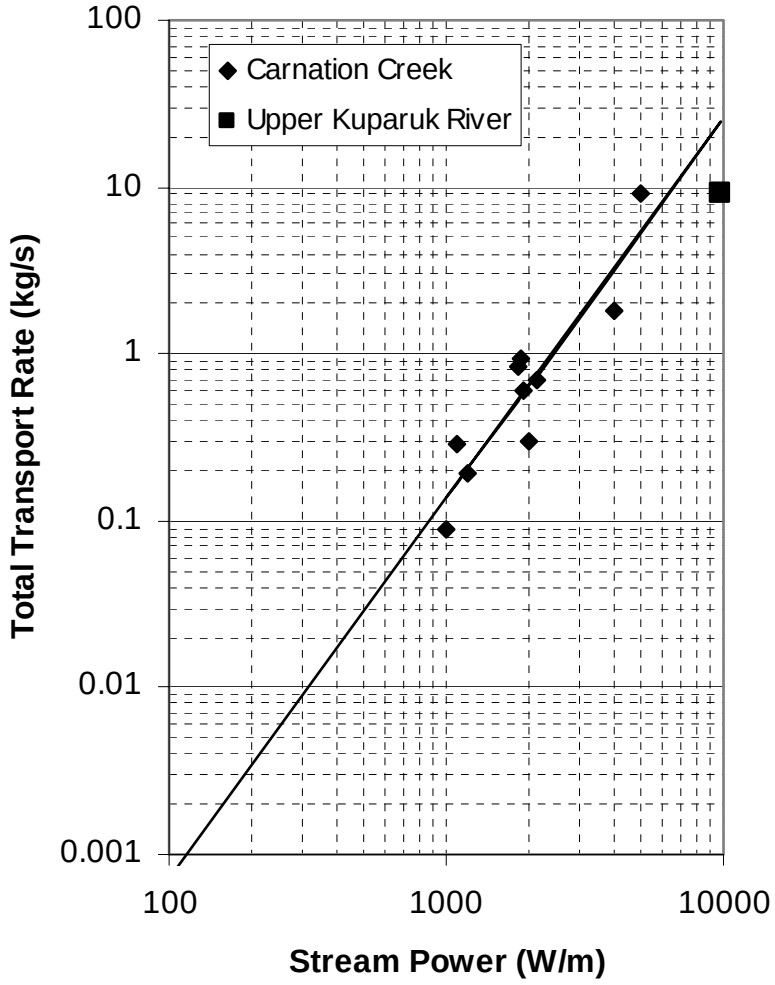

Figure 8.5 Transport rate vs. stream power for Carnation Creek, B.C., with the Upper Kuparuk River data point (Haschenburger and Church, 1998).

The image that best illustrates the geomorphic response is the plot of the water edge survey data shown in Figure 8.6. This figure shows both edges of the water, as well as the thalweg location, before and after the August 15th event. The initial survey data was obtained using a survey grade GPS unit on July 2nd, 2002. The post-event survey was performed on September 6th, 2002 using a total station. The discharge rates on these dates were approximately 4 and 6

m^3/s, respectively. Very little of the water edge difference can be attributed to the differences in discharge.

In addition, Figure 8.6 also identifies channel changes that will be looked at in more detail in the following section. These features will be examined in the order identified by the labels in this figure.

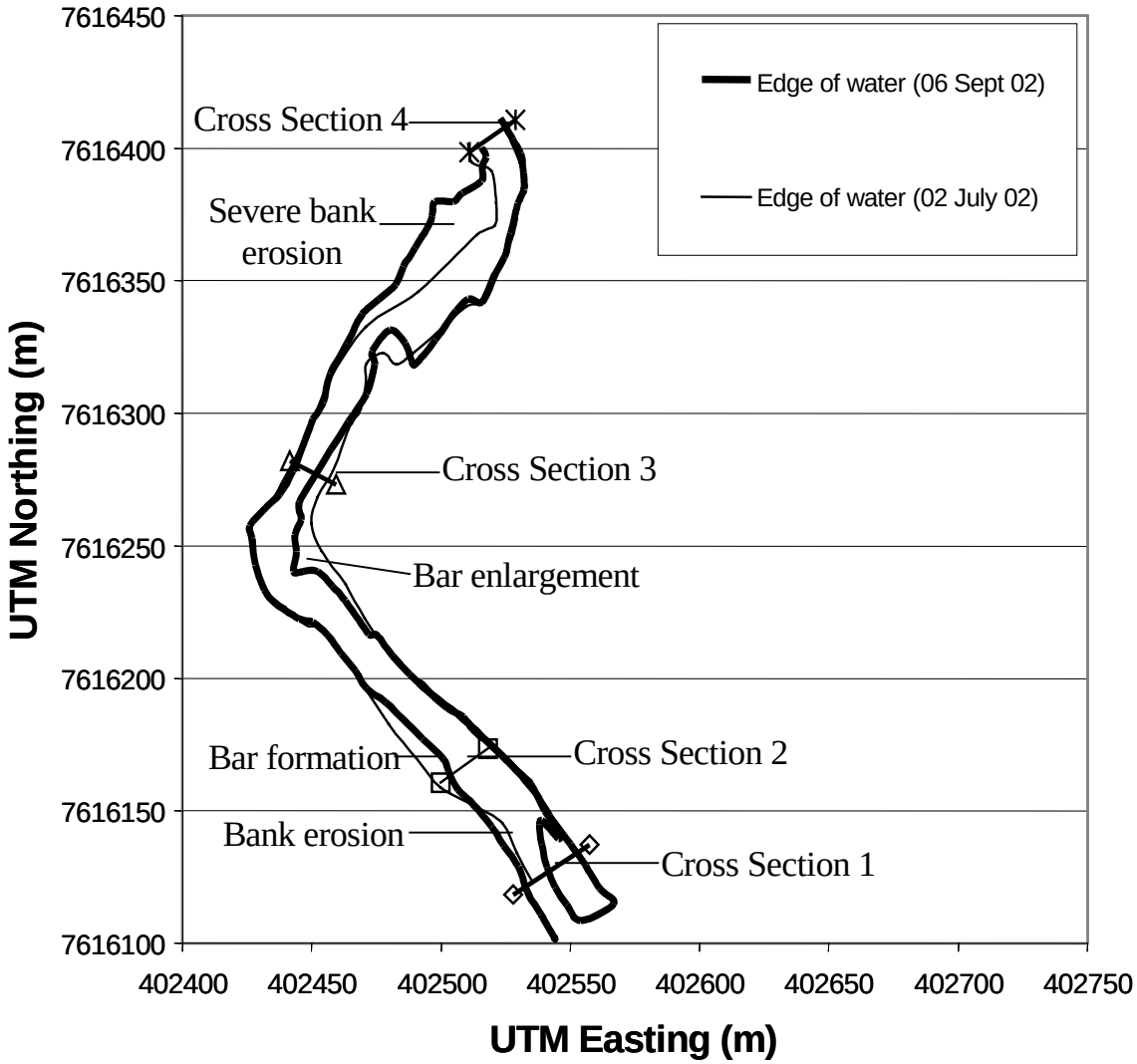

Figure 8.6 Map of pre- and post-event water edge surveys, also showing thalweg location changes.

Figure 8.7 shows the change in the longitudinal profile of the thalweg. This figure shows that practically the entire length of the thalweg was restructured. Linear trend lines through each set of data indicate that the reach-average slope was reduced slightly from 0.0075 to 0.0072.

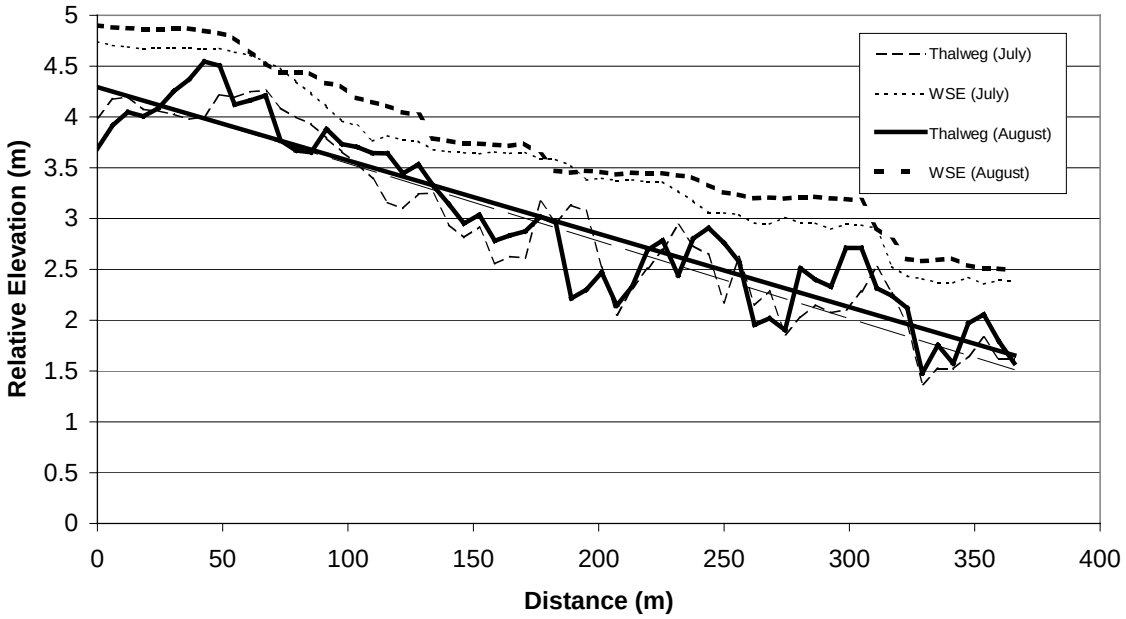

Figure 8.7 Pre- and Post event longitudinal profiles of the channel thalweg, with water surface level and linear fits of the channel profile data.

Feature 1: Cross Section 1

As Figure 8.8 shows, cross section 1 underwent significant changes during the event. The left bank was eroded by four meters, the thalweg was scoured by 0.28 meters and shifted towards the newly eroded left bank, and an existing bar on river right was aggraded by as much as 0.75 meters.

Both data surveys shown in Figure 8.9 were obtained during the summer of 2002. There is likely to be some amount of error associated with surveying channel cross sections, particularly when the bed material is as course as that of the Kuparuk River. The boulders and large void spaces cause some amount of difference from one survey to the next, even when no bedload transport has occurred. In Appendix VI are two pairs of cross sectional surveys with no bedload transport occurring between either set. Despite the fact there has been no movement, there is up to 19 cm of difference in the vertical elevations of the survey sets. It is unlikely that there is that much error capturing local maxima or minima, but in the regions between, there appears to be some error.

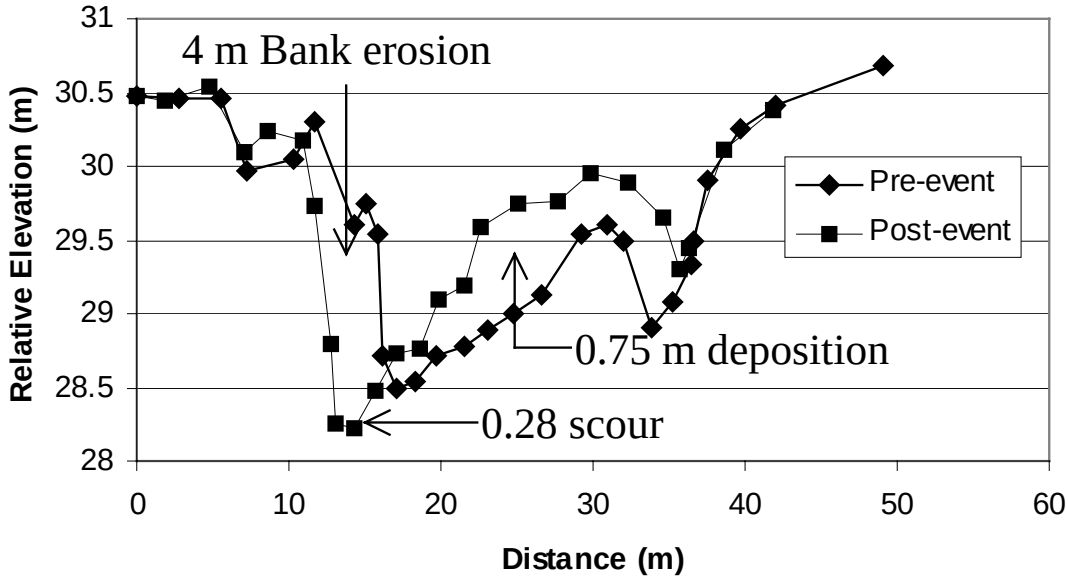

Figure 8.8 The change in cross section 1.

Feature 2: Cross Section 2

Cross section 2 was the initial location of the orange tracers. This section is located in a riffle. Typically riffles represent depositional regions and as Figure 8.9 shows, that was the case during this event. There was deposition across the

entire width of the cross section, with a large bar forming on river left that extended to the top of the left bank. This bar represents approximately 1.4 meters of aggradation.

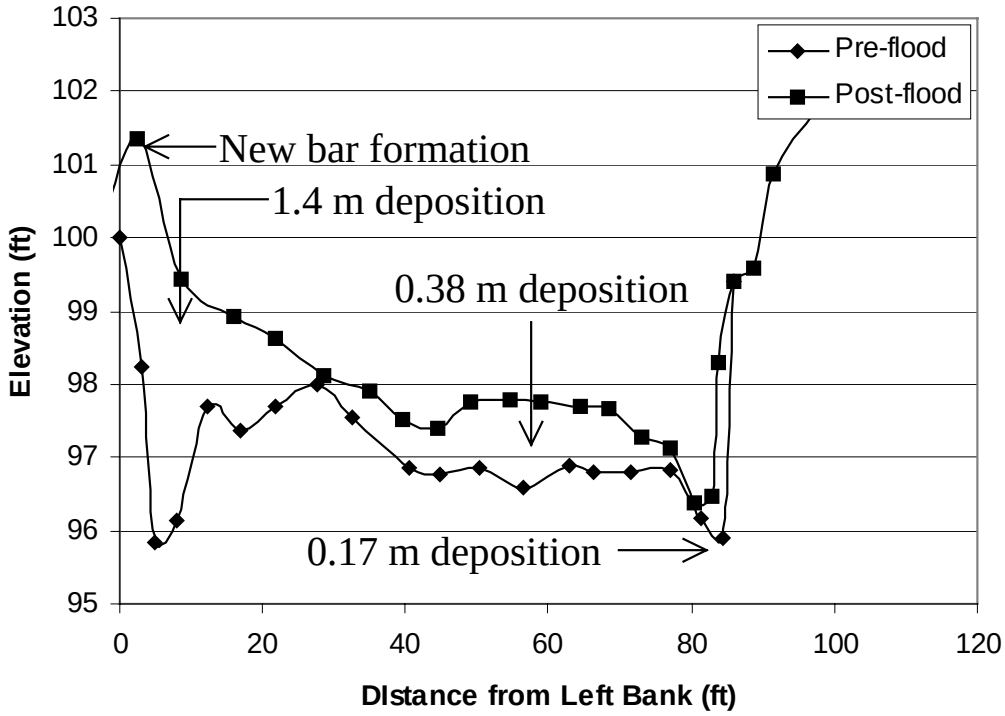

Figure 8.9 The change in cross section 2.

Feature 3: Cross Section 3

Cross section 3 was just below a sharp right hand bend in the channel. The left bank was stable through the event. There was some deposition in the thalweg, but most of the deposition occurred on the left bank where there was up to 0.58 meters of deposition (Figure 8.10).

Three scour chains on the left side of this cross section were buried deep enough that they could not be located with a metal detector. The detector is expected to

have a sensor depth of up to approximately 0.5 meter. It is possible that near the hydrograph peak, there was erosion in this cross section that was filled in during the falling limb. Thus, burying the scour chains deeper than the net aggradation.

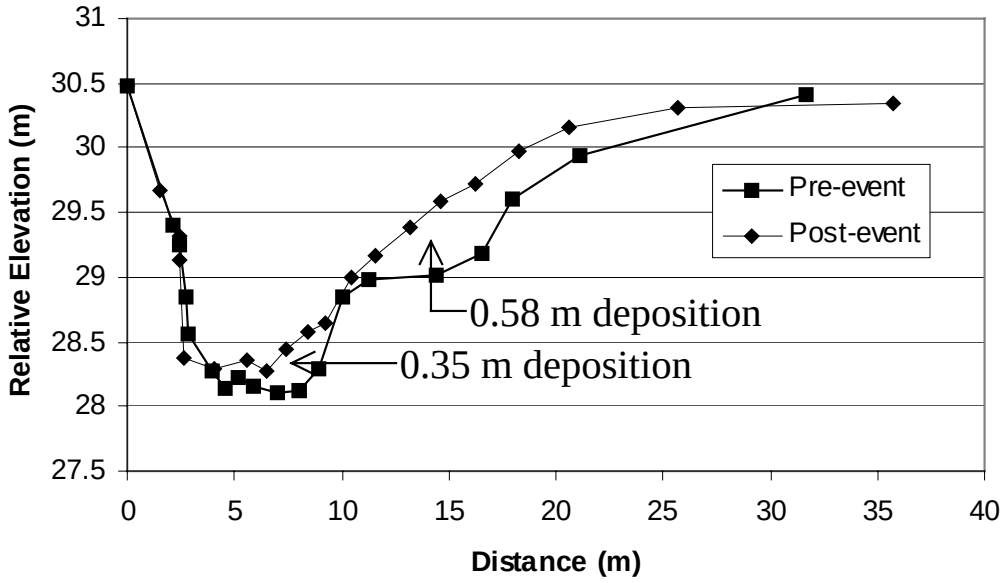

Figure 8.10 The change in cross section 3.

Feature 4: Cross Section 4

As Figure 8.11 illustrates, the left bank and thalweg of cross section 4 were both relatively stable. However, a scour chain located in the cross section was buried under cobbles and boulders up to 30 cm (median axis), indicating that the section was very active.

A large bar formed on the left side of the cross section. The area that the bar was formed in was above the active channel, or vegetation limit.

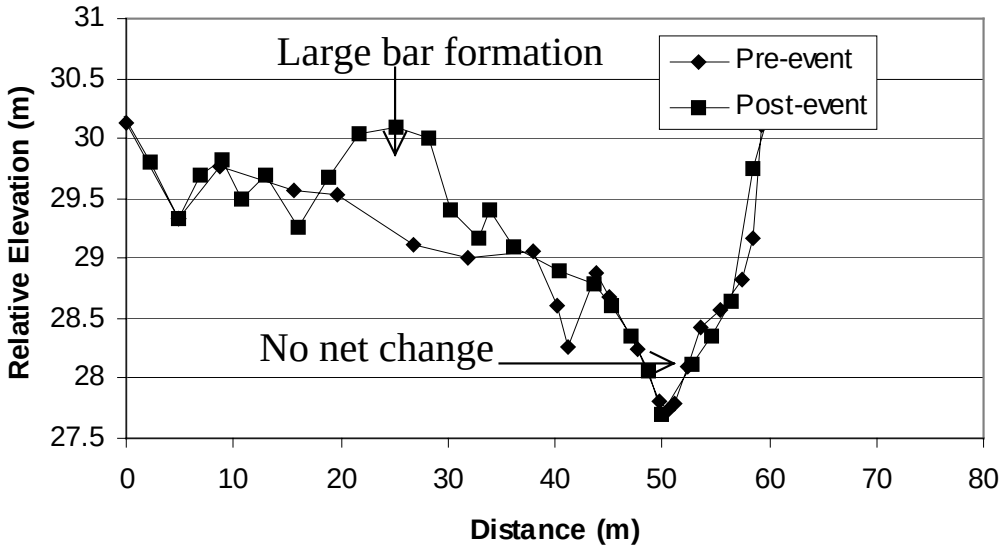

Figure 8.11 Changes in cross section 4.

Features 5, 6, and 7: Bank Erosion, bar formation, bar enlargement
These features are best illustrated by comparing the photographs shown in Figures 8.12 and 8.13.

Feature 5 is a significant amount of bank erosion on the left bank. The cross section 1 survey data showed that this amounted to approximately 4 horizontal meters of bank loss at that cross section.

Feature 6 is the formation of a bar on river left near cross section 2. The cross section 2 survey data showed that when this bar was formed a channel along the steep left bank was filled with more than 1.4 meters of material. As this bar reached the top of the left bank, a great deal of bed material was transported out of the channel and onto the overbank area. Figure 8.14 shows some of the material that was transported out of the channel.

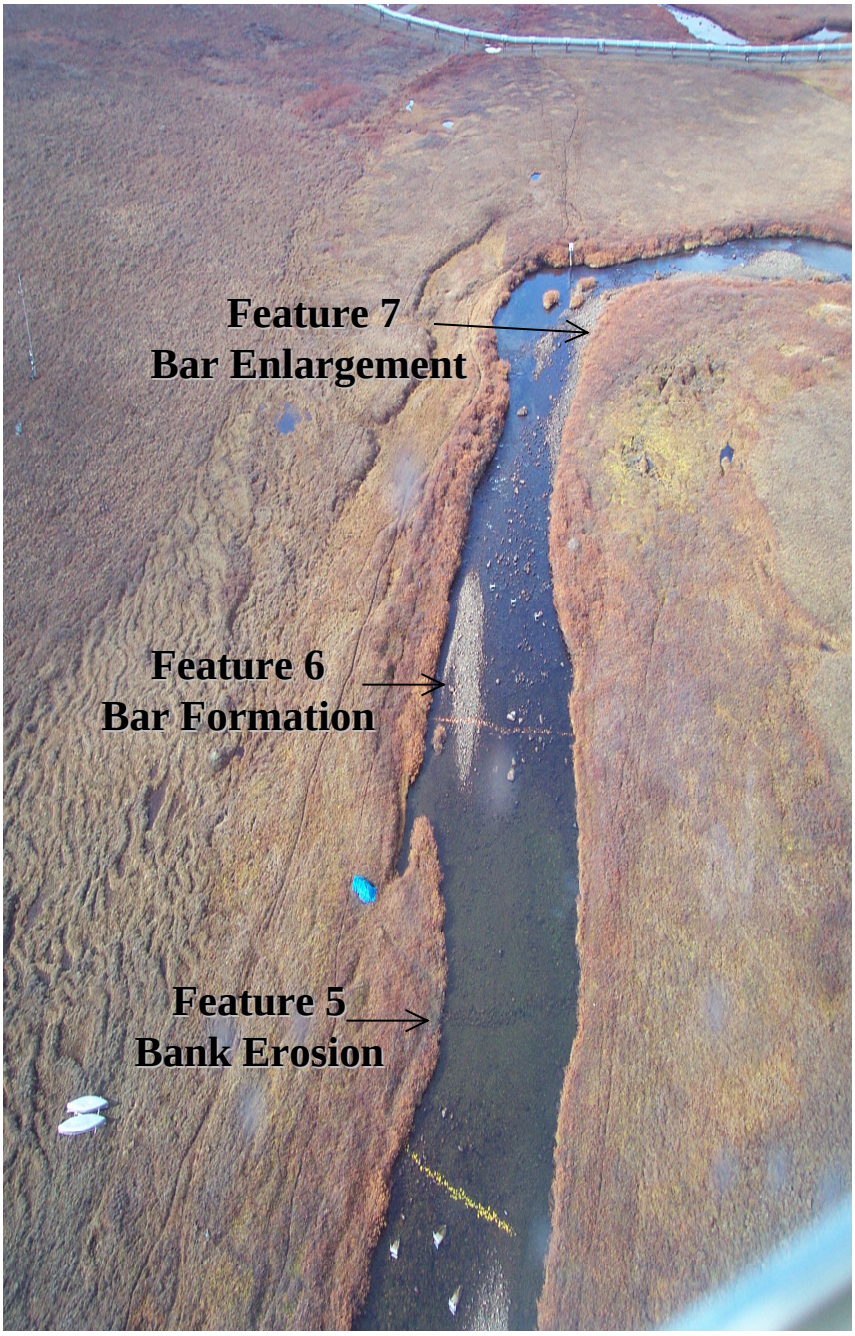

Figure 8.12 Pre-event photograph showing features 5, 6, and 7.

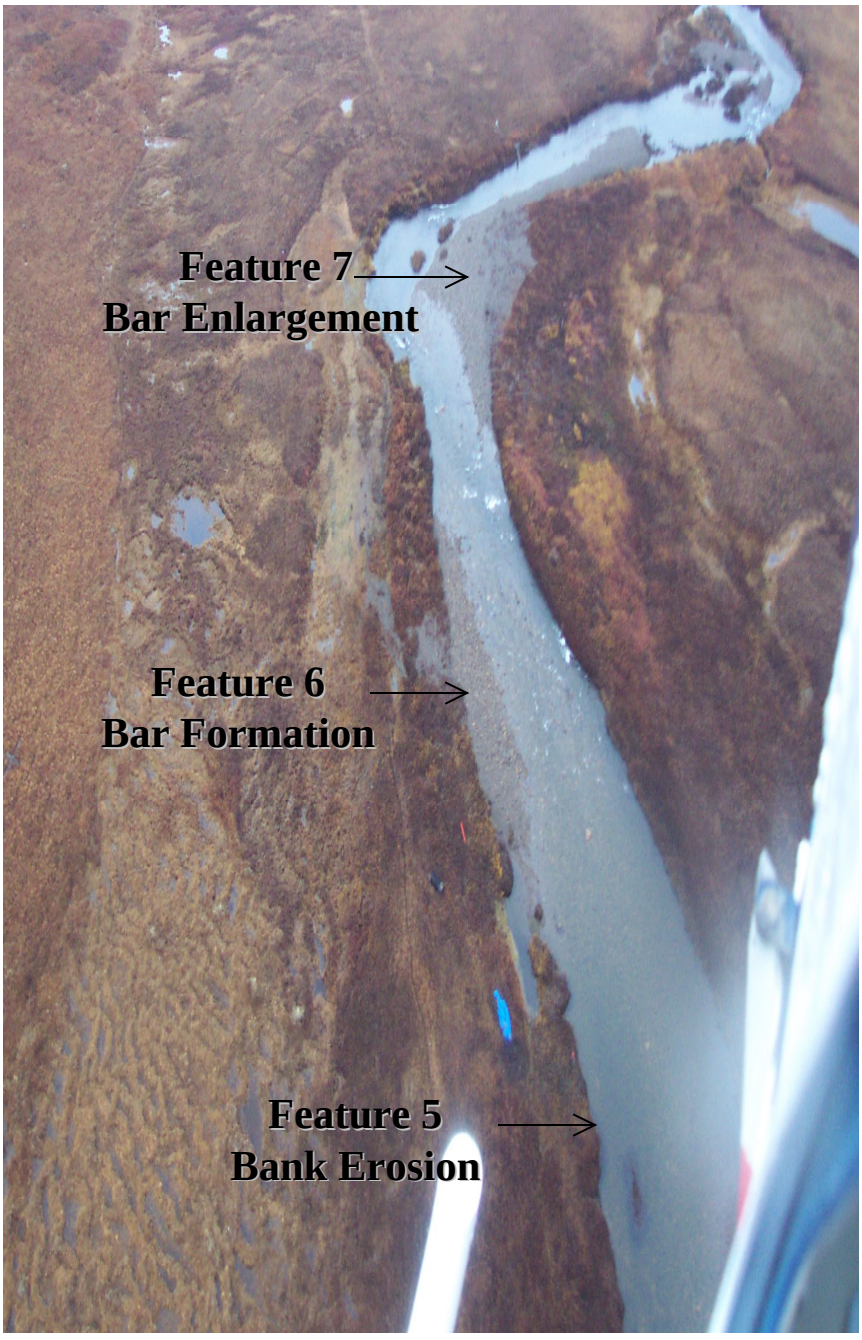

Figure 8.13 Post-event photograph showing features 5, 6, and 7.

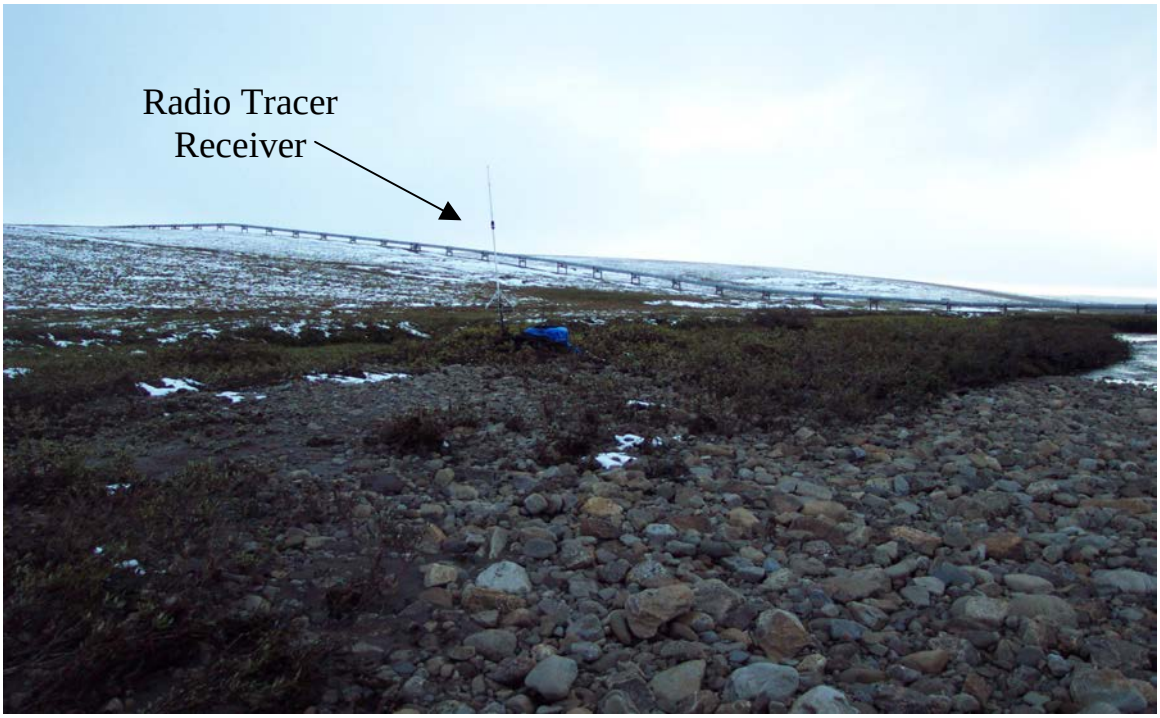

Figure 8.14 Bed material transported out of the channel near cross section 2.

Feature 7 is the enlargement of a bar on the inside of the right hand bend above cross section 3. The survey data for cross section 3 shows how much the bar height increased in that location. The photographs in Figures 8.12 and 8.13 show spatially how much larger this bar became during the event. These figures also show that there was deposition well above the vegetation limit on the right bank, with the vegetation limit still slightly visible in Figure 8.13.

Feature 8: Severe bank erosion

The left bank, on the inside of the left bend upstream from cross section 4 underwent the most significant change of the entire reach. In this section of the study reach, as much as 20 meters of lateral bank erosion occurred. Figure 8.15 shows photographs of this bend before and after the event. These photographs also show the large bar that was discussed in association with cross section 4.

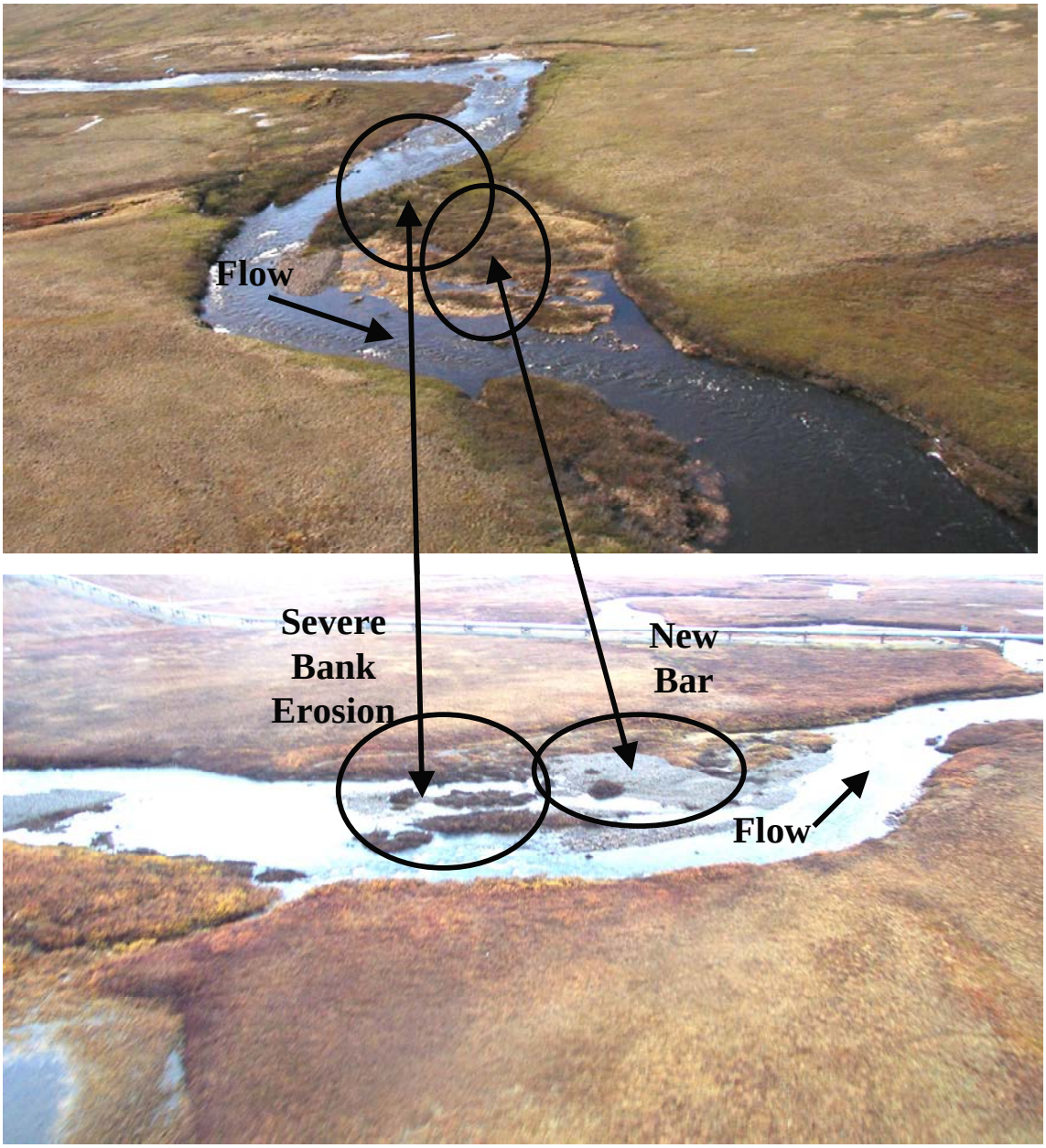

Figure 8.15 Severe bank erosion upstream from cross section 4. The top photograph was taken in 2001. The bottom photograph was taken after the August 2002 event.

Feature 9: Subsurface grain size

As described in section 4.1.5, a surface and subsurface grain size distribution was determined on the top of the bar in cross section 1 in July of 2002. The event provided an opportunity to repeat the survey to investigate the potential effects of the event on the sediment supply of the study reach. The results of these surveys are shown in Figure 8.16.

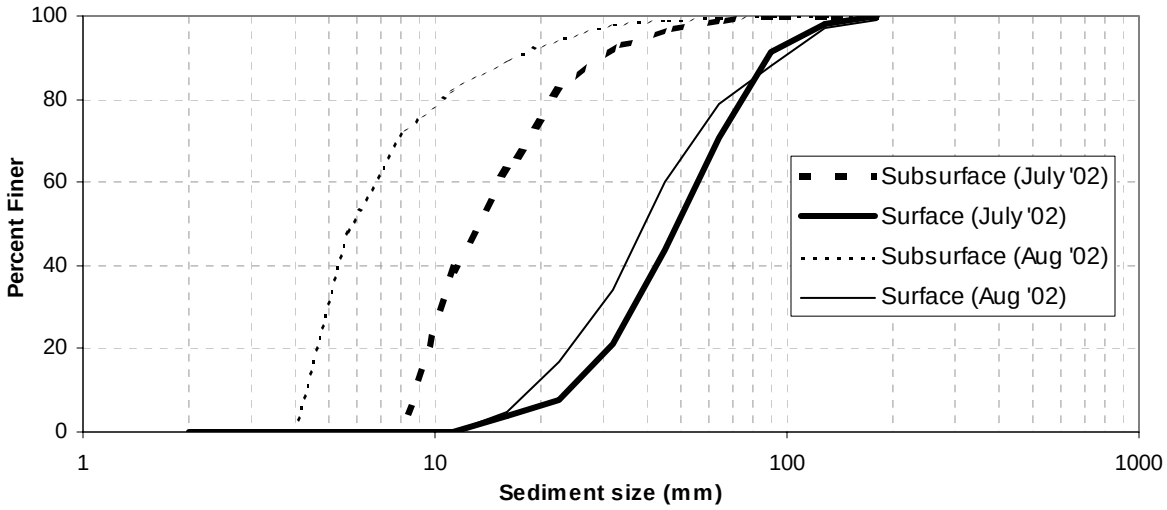

Figure 8.16 Surface and subsurface cumulative grain size distributions for cross section 1.

This figure shows that the surface grain size d_{50} decreased from 49 mm to 40 mm, and that the subsurface d_{50} decreased from 13.2 mm to 5.8 mm.

Calculated according to equation 7.3, the dimensionless transport capacity, q^*, was increased from a value of 0.29 in July to a value of 0.37 in August. This indicates that the sediment supply was increased by this event.

This calculated increase in sediment supply is consistent with observations made in the field. Prior to the event there was little small gravel material among the course, cobble-sized material, particularly in the riffle sections. Immediately following the event there was more small material filling void spaces among the larger bed materials. The condition is likely a result of winnowing of the fine material that occurs over time, leaving a course armor layer on the bed surface.

8.4 Terrain Maps

In July of 2002, a survey-grade GPS unit was used to thoroughly survey the topography of the study reach to generate a terrain map. After the event occurred the survey was repeated using a total station to generate a map that could be compared to the first. These maps are shown in Figures 8.17 and 8.18.

Visually there are some differences, but perhaps not as significant as expected given the geomorphic changes that have already been discussed. However, when these two data sets were grided, and the grid values differenced, a map of the changes in elevation was generated. This map is shown in Figure 8.19.

Although there are places were the survey resolution does not do an adequate job of capturing the channel and bank topography, this difference map better shows the changes that took place in the study reach. This is particularly true of the bank erosion in cross section 1 and upstream of cross section 4, and the bar enlargement in the vicinity of cross section 3. The bar formed in cross section 2 appears to be under-represented by this data. The two survey data sets are shown in Appendix VII.

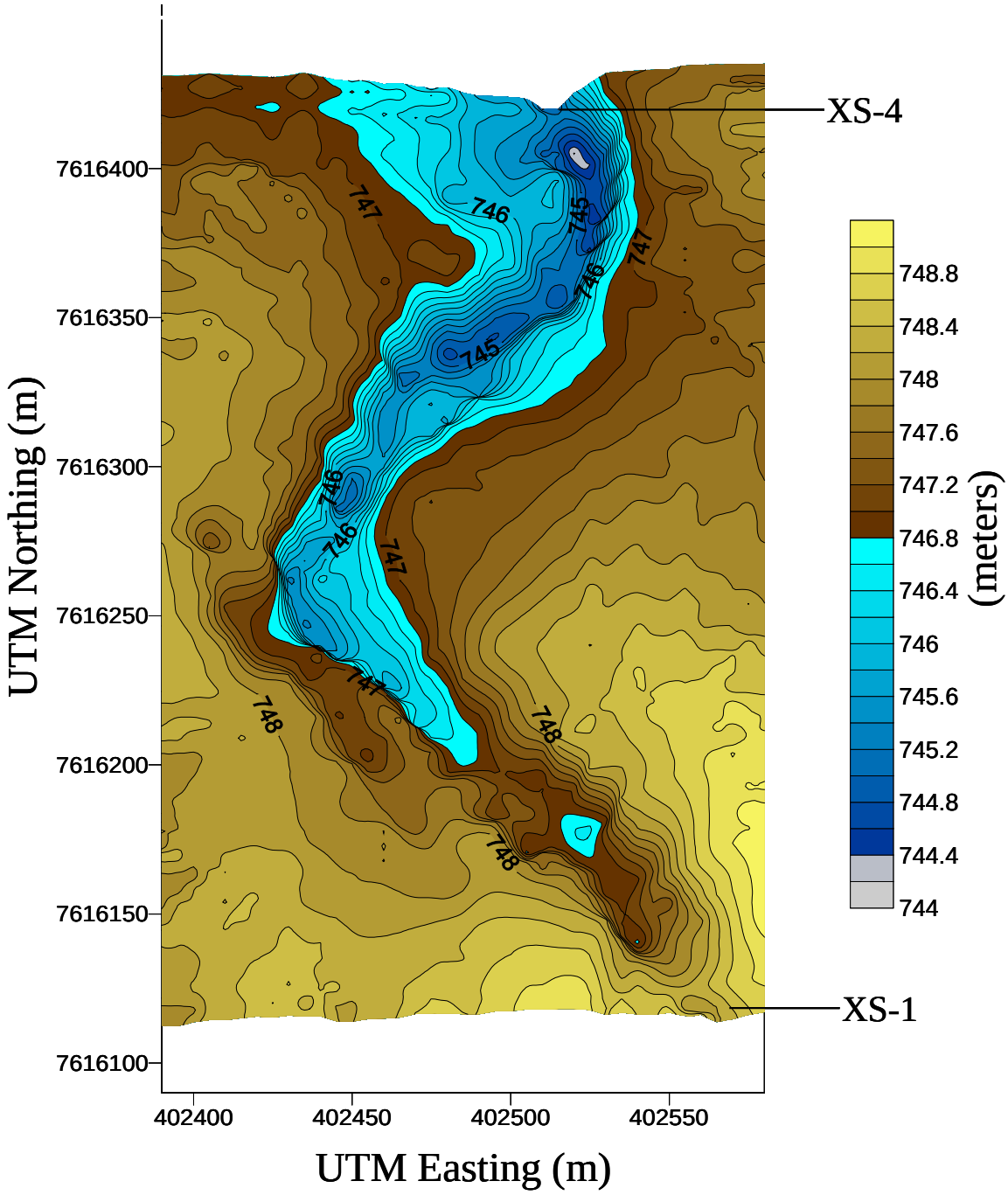

Figure 8.17 Pre-event terrain map of the study site.

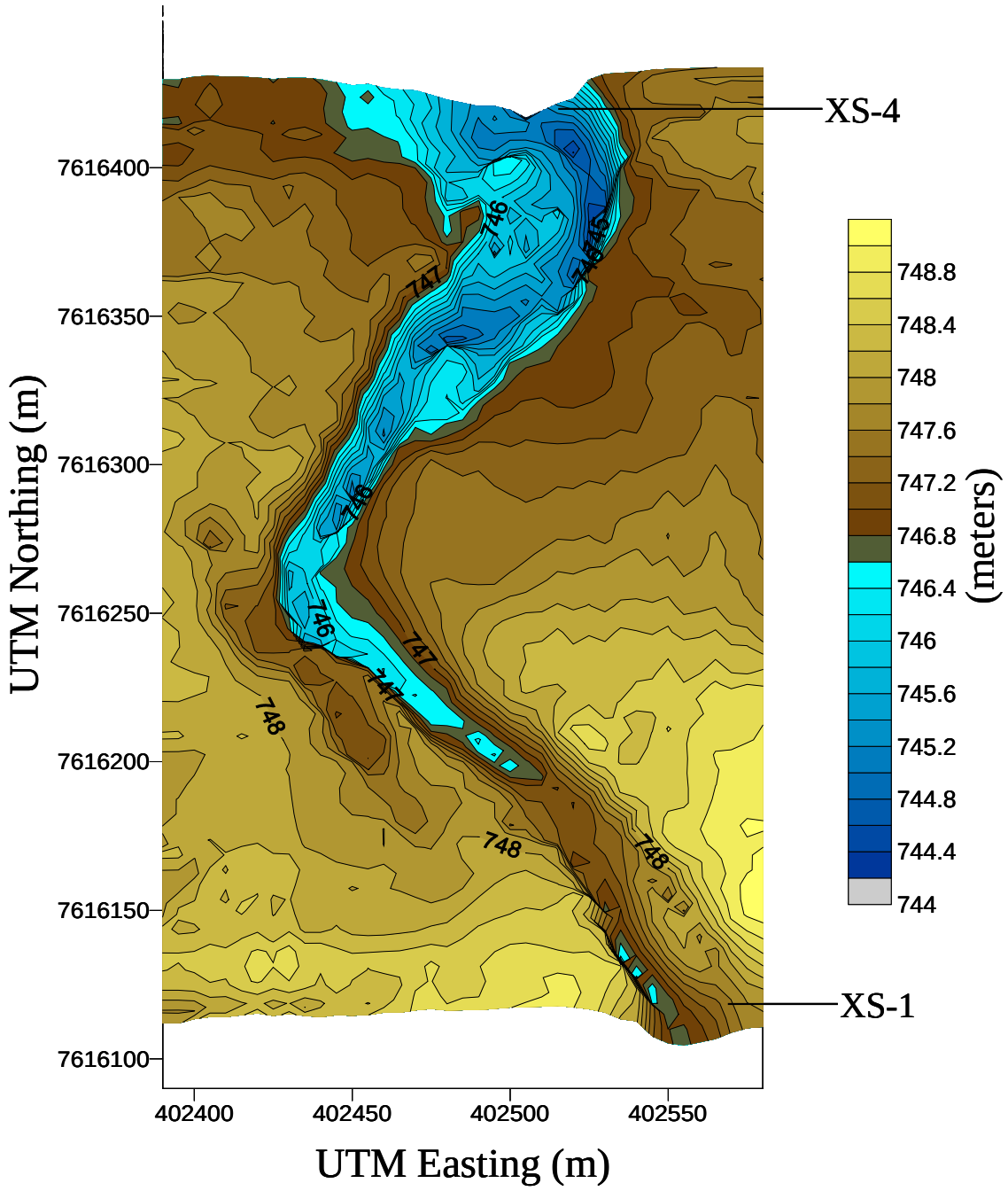

Figure 8.18 Post-event terrain map of the study site.

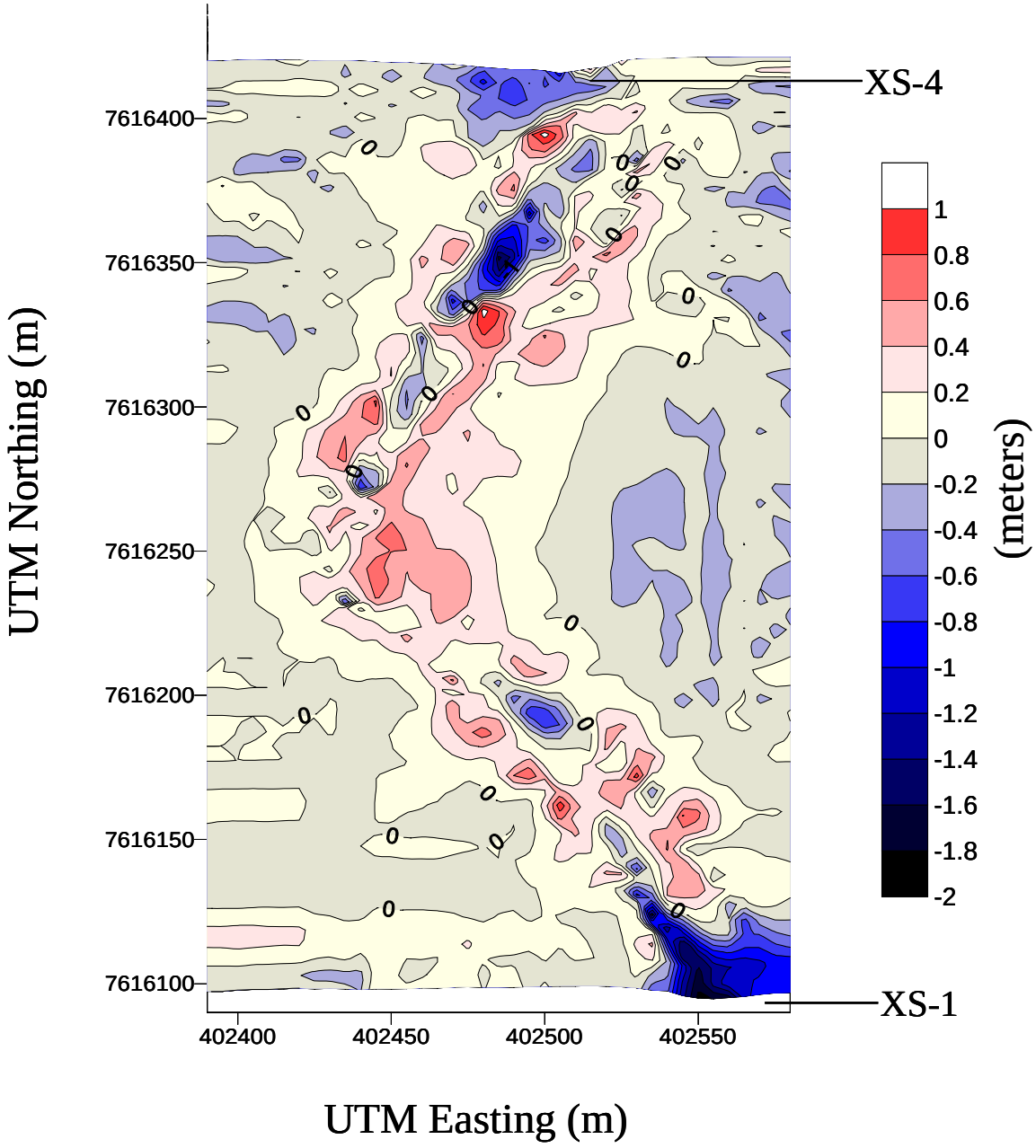

Figure 8.19 Map of the change of elevation determined by subtracting the pre-event surface from the post-event surface for the study site.

9. Conclusions

The analysis done in Chapter 6 indicates that in the Upper Kuparuk River, over the ten-year period from 1993 to 2002, a significant amount of bedload transport was suppressed due to the presence of bottom ice during the snowmelt runoff period.

During this period, competent flows, with the potential to generate a significant amount of bedload movement, occurred six times. Three of these events (1993, 1999, 2002) were due to summer rainfall, or rain-on-snow events. The 1999 and 2002 events both resulted in significant morphological changes to the study reach. Nothing is known about the 1993 event. The other three competent events (1996, 1997, 2000) occurred during snowmelt runoff when the bottom ice presence prevented any significant bedload movement.

Due, at least partly to the presence of bottom ice during the snowmelt runoff period, the dominant discharge, or channel forming or maintaining discharge, appears to be related to the large summer events, such as those of August 2002, and July 1999. The August 2002 event created a tremendous morphological response in the study reach with the formation of new bars, modification of existing bars, significant scour, and a large amount of bank erosion.

Analysis of the tracer rock movement data obtained during this rain-on-snow event, which had a peak discharge of approximately 98 m^3/s, indicates that an estimated 870 m^3 of bed material moved in the study reach.

The total amount of lost bedload transport potential was calculated to be between 50,000 m^3 and 50,000,000 m^3 for the three cross sections located in pools, and 500 m^3 for the cross section located in a riffle. This is obviously an unrealistically large discrepancy and the actual value would likely be somewhere between the lower and upper values.

When the August 2002 event was analyzed using the bedload rating curve method the results closely matched the tracer rock calculations for cross section 2 (riffle). The average bedload transport, estimated using tracer rock data, was determined to be 9.1 kg/s. Using the bedload rating curves, the Parker equation predicted an average value of 16.5 kg/s and the Meyer-Peter and Mueller method predicted an average value of 33.6 kg/s.

Given the random and variable nature of bedload transport, these predictions should be considered to be order-of-magnitude estimates. However, for this event the two methods appear to correlate well. This comparison suggests that the 50,000 and 50,000,000 m^3 predictions are gross overestimates of the potential bedload transport, and the value is likely to be closer to the 500 m^3 of material predicted for the riffle cross section.

This indicates that the total amount of bedload transport not realized over the ten-year record is, conservatively, comparable to the amount that occurred during the largest single summer event over this same period.

It is difficult to predict what this means in terms of channel morphology, because a single large event is fundamentally different than a series of smaller events. However, it is reasonable to expect that over longer time scales, this is a significant factor in the evolution of the river system.

There are deficiencies to this analysis that should be addressed. One of the biggest weaknesses is that this study relies on only ten years of data. This is not long enough to characterize hydrologic trends. After the 1999 rainfall event, which peaked at approximately 84 m^3/s, more than three times any previous value, it was believed that such an event was a rare occurrence. However, the August 2002 event suggests that may not be the case.

When discussing the dominant discharge of a gravel bed river, which would typically see significant bedload movement infrequently, having a ten-year record is a limitation. During the available record, 50% of the major events (25 m^3/s or greater) occurred during snowmelt runoff. How this trend continues over a 50 or 100-year period will better define how the suppression of bedload transport by bottom ice affects the dominant discharge of the study site. Over the next 10 or 20 years, the probability of another event of the magnitude of the August 2002 may be low, relative to the probability of several 25 m^3/s snowmelt events occurring. If that were to be the case, the affect of ice on the dominant discharge would be more clearly identified over that time scale.

Perhaps a larger statistical concern than the lack of discharge history is the observation of only one competent event. Particularly since that event was so large that it completely mobilized the bed and resulted in only a 13% recovery rate of tracer particles. This analysis relies largely on the ability of the selected bedload transport equations to accurately predict transport rates. Given the variable nature of bedload transport, a data point closer to the threshold value would add a great deal of confidence to the analysis.

9.1 Future Work

In Chapter 1, the idea that bottom ice can also promote bedload transport, through ice rafting and localized scour, was introduced. Three seasons of

observations on the Upper Kuparuk River supports the belief that these are valid mechanisms, but that they are orders of magnitude less significant than the potential for bedload transport in an ice-free channel. Scour chain data, and channel cross section surveys performed immediately following the snowmelt runoff period, indicate that bedload transport during this event is insignificant.

However, it is not known whether this is true for the entire length of the river that experiences bottom ice. The belief is that this is valid throughout the extent of bottom ice, but there are no observations to support this position. Studies of the sedimentation processes in different regions of the river could be useful in substantiating these beliefs.

Another topic that certainly deserves consideration is how permafrost may affect these processes, particularly with respect to bank erosion. McNamara (1999, 2001) has demonstrated that river systems of the Arctic exhibit a tendency towards being underdeveloped. While the suppression of the bedload transport by bottom ice has been shown to play a role in this condition, permafrost likely plays a role as well.

It is likely that had the event of August, 2002 occurred earlier in the season, there would have not been nearly as great of a geomorphic response because the banks, and at some depth the bed, would have been better protected by frozen ground.

Developing a better understanding of the roles permafrost and ice play in arctic river morphology will result in an improved ability to understand the affect of a changing climate on these systems.

10. References

Best, H. R., 2002. The influence of ice on channel morphology of the Kuparuk River, Alaska: A master's thesis. Boise State University.

Buffington, J. M., Montgomery, D. R., 1997. A systematic analysis of eight decades of incipient motion studies, with special reference to gravel-bed rivers, Water Resources Research, 33(8): 1993-2029.

Bunte, K., 2001. Measuring gravel and bedload transport rates and initiation of motion using portable traps. Proceedings of the 7th Federal Interagency Sedimentation Conference, Reno, Nevada, III-24.

Chacho, E.F., Jr., Burrows, R.L., Emmett, W.W., 1989. Detection of course sediment movement using radio transmitters. Proceedings of the XXIII Congress of the International Association for Hydraulic Research, The National Research Council of Canada, B367-B373.

Dietrich, W. E., Kirchner, J.W., Ikeda, H., and Iseya, F., 1989. Sediment supply and the development of a course surface layer in gravel-bedded river, *Nature*, 340: 215-217.

Dingman, S. L., 1994. Physical hydrology, Macmillan publishing company, New York, 650 pp.

Einstein, H. A., 1950. The bed-load function for sediment transportation in open channel flows, U.S. Department of Agriculture, Soil Conservation Service, Technical Bulletin no. 1026.

Emmett, W. W., Burrows, R. L., Chacho, E. F., Jr., 1996. Course-particle transport in a gravel-bed river, International Journal of Sediment Research, 11(2): 8-20.

Emmett, W. W., Wolman, M. G., 2001. Effective discharge and gravel-bed rivers, Earth Surface Processes and Landforms, 26: 1369-1380.

Furgeson, R.I., Wathen, S.J., 1998. Tracer-pebble movement along a concave river profile: Virtual velocity in relation to grain size and shear stress, Water Resources Research, 34(8): 2031-2038.

Hinzman, L.D., and Kane, D.L., 2001. Meteorological and hydrological data, Kuparuk River Nested Watershed Study. University of Alaska Fairbanks, Water and Environmental Research Center. Digital media.

Haschenburger, J.K., Church, M., 1998. Bed material transport estimated from the virtual velocity of sediment, Earth Surface Processes and Landforms, 23: 791-909.

Hassan, M. A., Church, M., 2001. Sensitivity of bedload transport in Harris Creek: seasonal and spatial variation over a cobble-gravel bar, Water Resources Research, 27(3): 813-825.

Hodel, K. L., 1986. The Sagavanirktok River, North Slope Alaska: characterization of an arctic stream, The United States Geological Survey, open file report 86-267, 28 pp.

Kane, D.L., Hinzman, L.D., McNamara, J.P., Zhang, Z., Benson, C.S., 1999. An overview of a nested watershed study in Arctic Alaska, Nordic Hydrology, 31(4/5): 245-255.

Kempema, E.W., Reimnetz, E., Clayton, J.R. Jr., Payne, J.R., 1993. Interactions of frazil and anchor ice with sedimentary particles in a flume, Cold Regions Science and Technology, vol. 21: 137-149.

Knighton, D., 1998. Fluvial forms and processes, a new perspective. Oxford University Press Inc, New York, 383 pp.

Leopold, L. B., 1992. Sediment size that determines channel morphology. Dynamics of gravel-bed rivers, Wiley, Chichester, pages 297-307.

Leopold, L. B., Wolman, M. G., Miller, J. P., 1964. Fluvial processes in geomorphology. W. H. Freeman and Company, San Francisco, 493 pp.

Martini, I.P., Kwong, J.K., Sadura, S., 1993. Sediment ice rafting and cold climate fluvial deposits: Albany River, Ontario Canada, special publications International Association for Sedimentation, 17: 63-76.

McNamara, J. P., Kane, D. L., Hinzman, L. D., 1997. Hydrograph separations in an arctic watershed using mixing model and graphical techniques, Water Resources Research, 33(7): 1707-1719.

McNamara, J. P., Kane, D. L., Hinzman, L. D., 1999. An analysis of an arctic channel network using a digital elevation model, Geomorphology, 29: 339-353.

McNamara, J.P., 2000. Bankfull flow, hydraulic geometry, and river ice in a northern river; AWRA conference proceedings: Water Resources in Extreme Environments; Kane, D.L. (ed.), Anchorage, Alaska, p. 191-196.

McNamara, J.P., (in review: Hydrological Processes). Using motion-sensing radio transmitters to observe incipient motion and transport hysteresis of course gravel.

Osterkamp, T.E., Payne, M.W., 1981. Estimates of permafrost thickness from well logs in northern Alaska, Cold Regions Science and Technology, 5 (1), 13-27.

Parker, G., 1990. The ACRONYM series of Pascal programs for computing bedload transport in gravel rivers, *SAFL External Memo No. M-220*.

Rosgen, D.L., 1994. A classification of natural rivers. Catena, 22, 199 pp.

Ryan, S. E., Troendle, C. A., 1997. Measuring bedload in course-grained mountain channels: Procedures, problems, and recommendations; Water resources education, training, and practice: Opportunities for the next century, American Water Resources Association, pp 949-958.

Schmidt, K. H., Ergenzinger, P., 1992. Bedload entrainment, travel lengths, step lengths, rest periods – studied with passive (iron, magnetic) and active (radio) tracer techniques, Earth Surface Processes and Landforms, 17: 147-165.

Scott, K. M., 1978. Effects of permafrost on stream channel behavior in arctic Alaska, United States Geological Survey Professional Paper 1068, 19 pp.

Smith, D.G., 1979. Effects of channel enlargement by river ice processes on bankfull discharge in Alberta, Canada, Water Resources Research, 15(2): 469-475.

Syvitski, J. P.M. (in review: Polar Research). Sediment transport variability in arctic rivers: implications for a warmer future.

Terada, K., Hirayama, K., Sasamoto, M., 1999. Field measurements of anchor and frazil ice, Ice in surface waters, Shen (ed.), Balkema, Rotterdam, pages 697-702.

Wilcock, P. R., 1997. Entrainment, displacement and transport of tracer gravels, Earth Surface Processes and Landforms, 22: 1125-1138.

Woo, M. K., Sauriol, J., 1981. Effects of snow jams on fluvial activities on the High Arctic, Physical Geography, 2: 83-98.

Yang, C. T., 1996. Sediment Transport: Theory and practice. McGraw-Hill, New York, 396 pp.

Appendix I: Upper Kuparuk river gauge site annual hydrographs

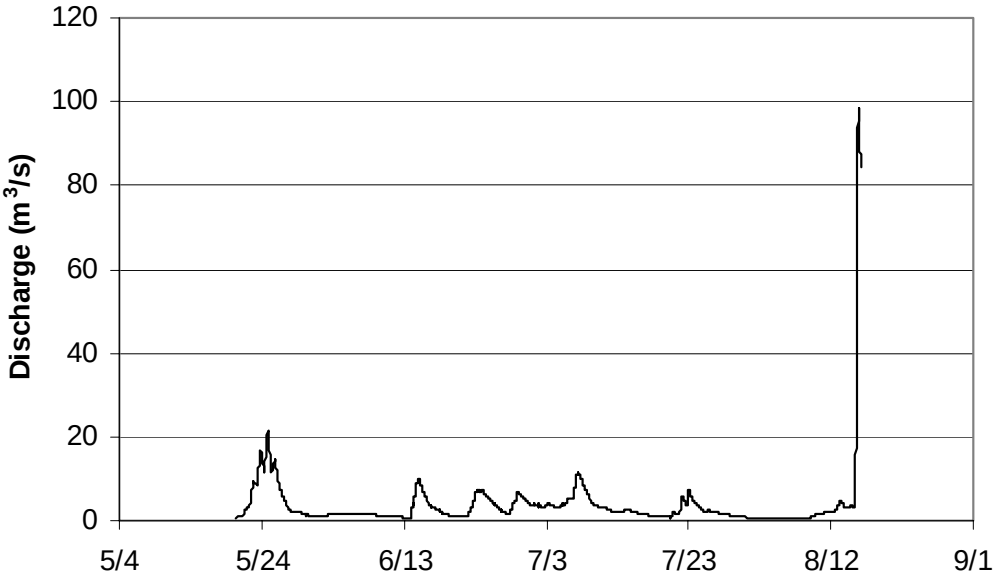

Figure A1.1 2002 Upper Kuparuk hydrograph.

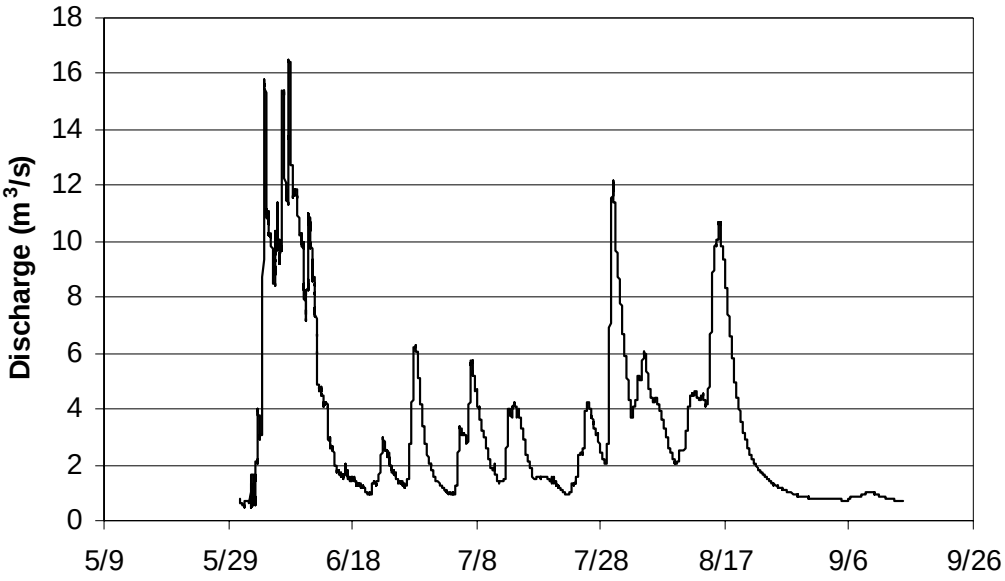

Figure A1.2 2001 Upper Kuparuk hydrograph

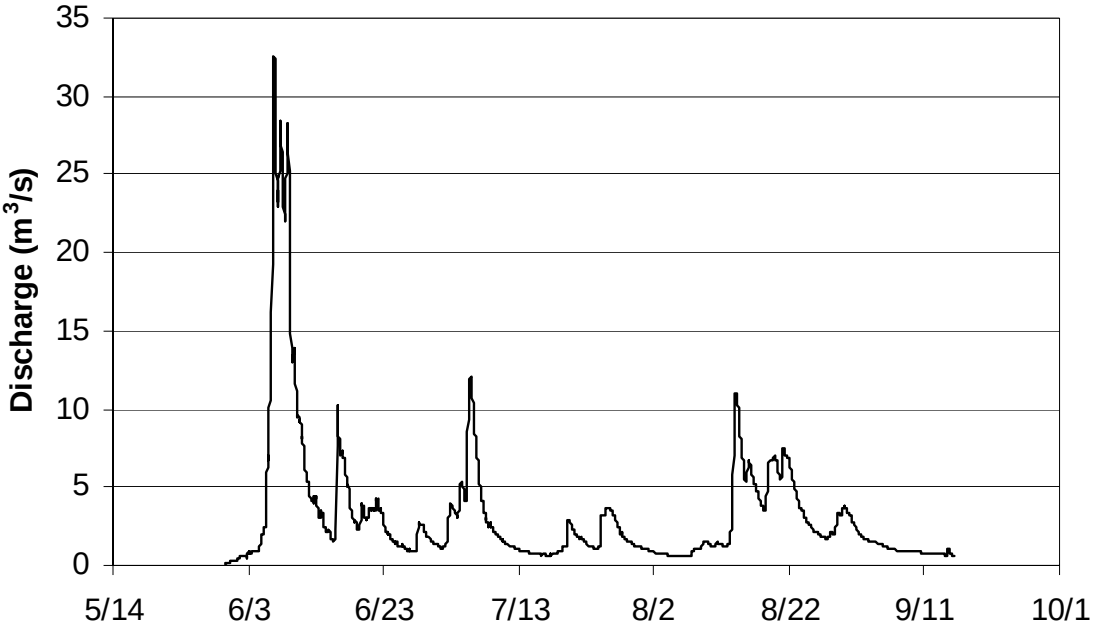

Figure A1.3 2000 Upper Kuparuk hydrograph

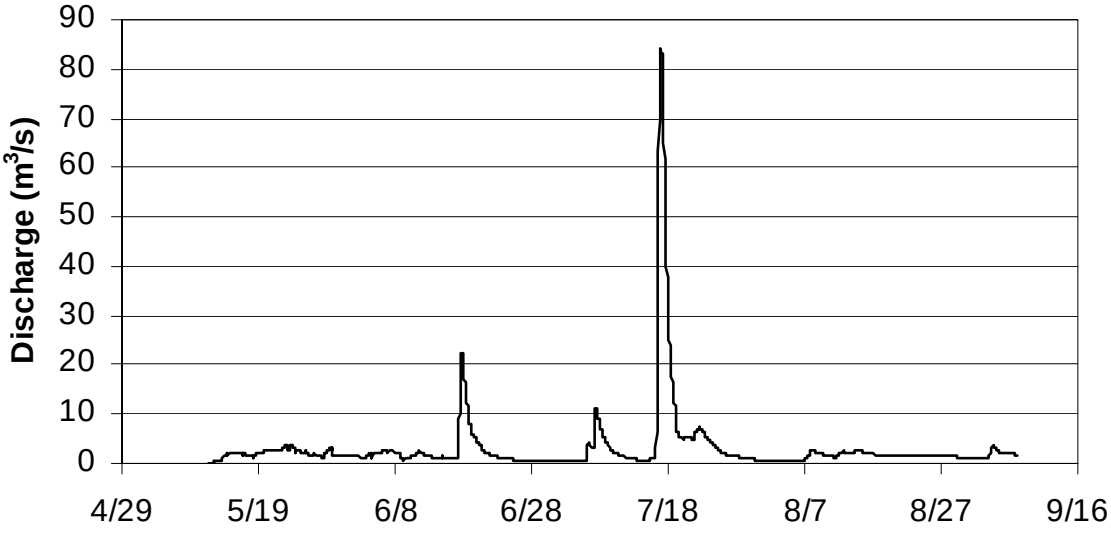

Figure A1.4 1999 Upper Kuparuk hydrograph

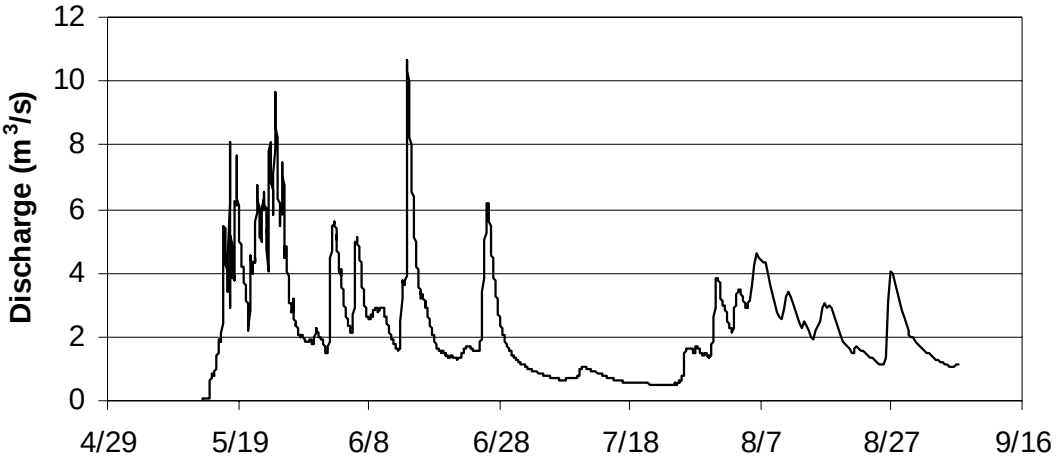

Figure A1.5 1998 Upper Kuparuk hydrograph

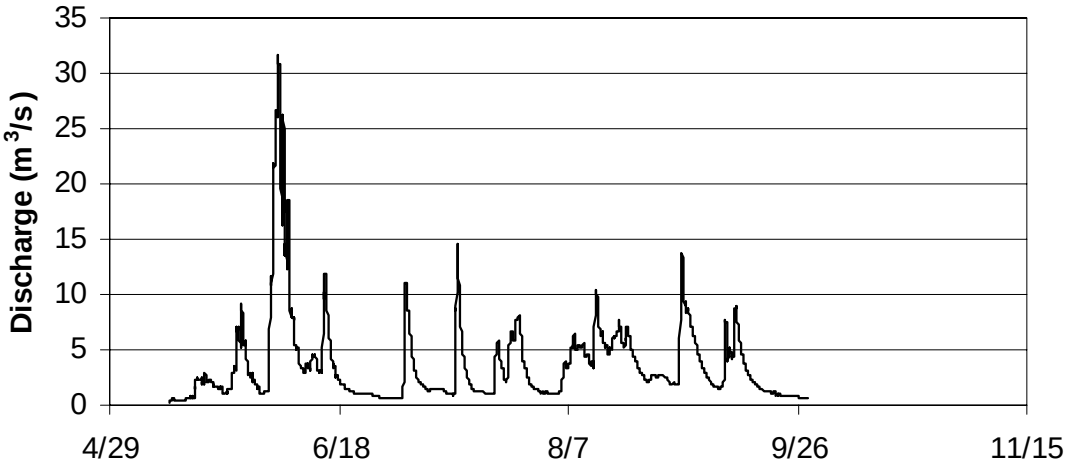

Figure A1.6 1997 Upper Kuparuk hydrograph

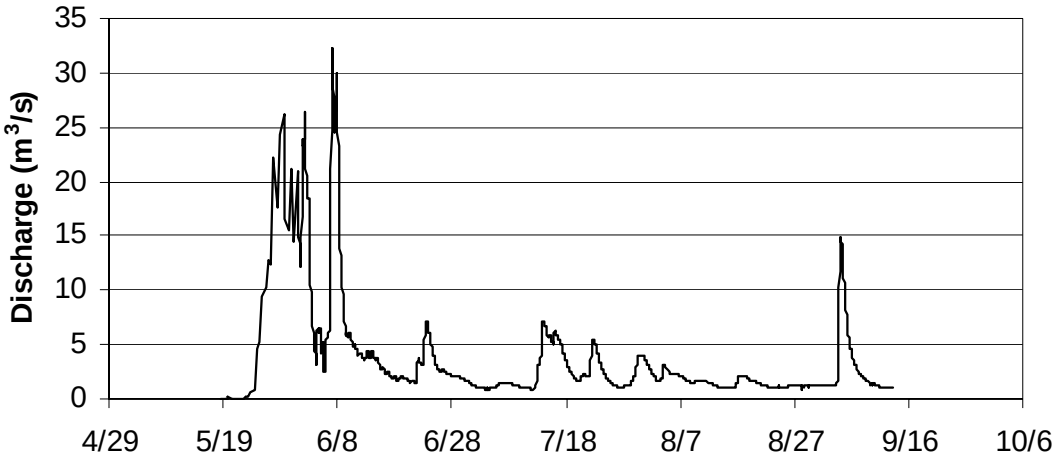

Figure A1.7 1996 Upper Kuparuk hydrograph

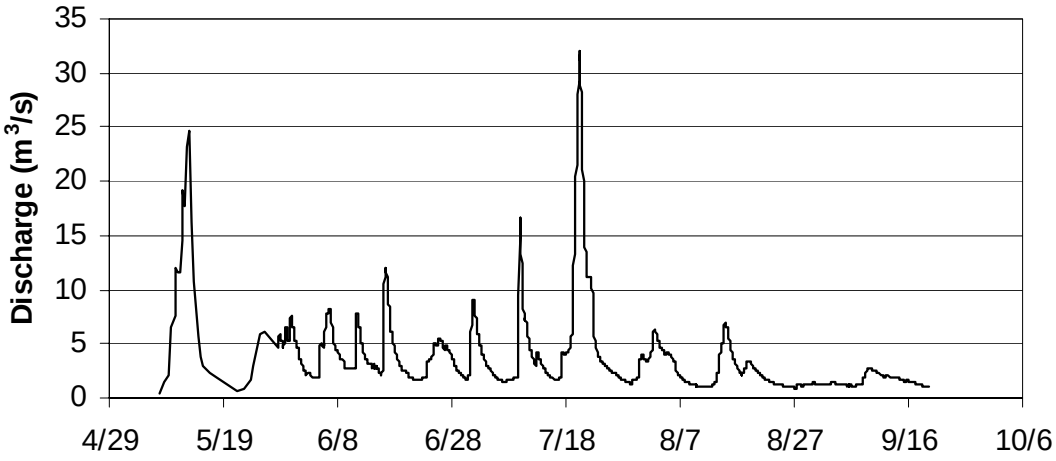

Figure A1.8 1995 Upper Kuparuk hydrograph

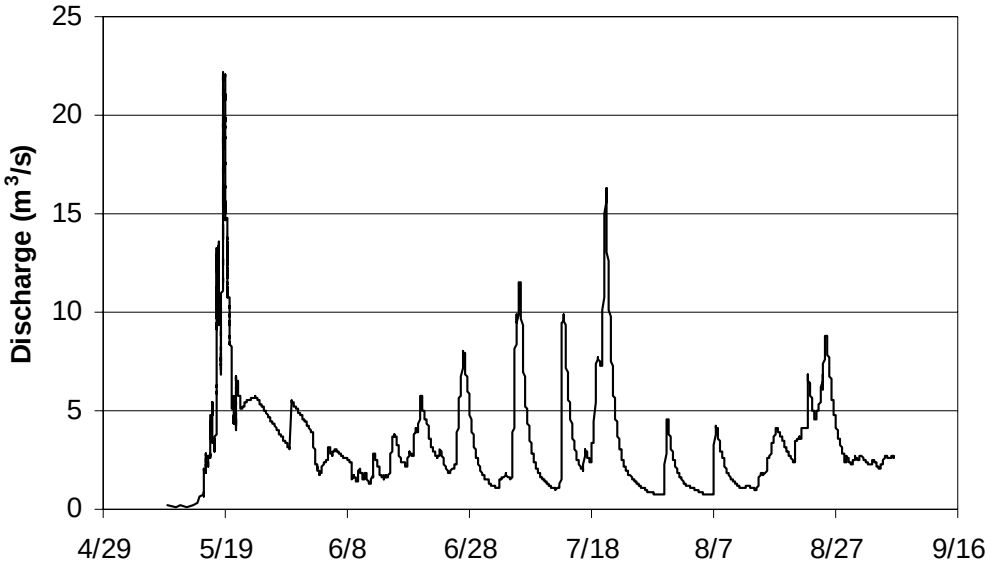

Figure A1.9 1994 Upper Kuparuk hydrograph

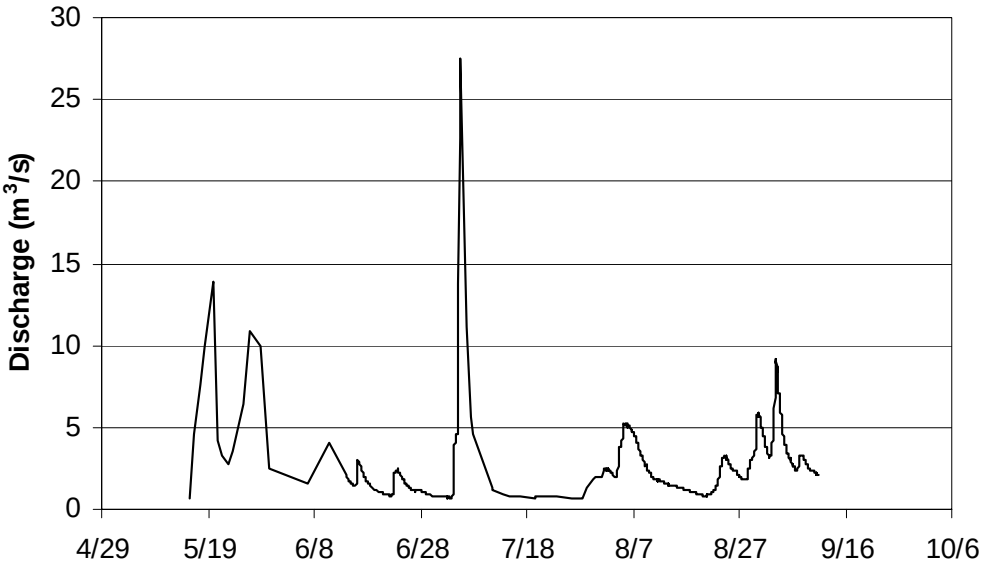

Figure A1.10 1993 Upper Kuparuk hydrograph

Appendix II: Sediment Traps

Figure A2.1 Photograph of a sediment trap clogged with organic material, from the Upper Kuparuk River study site (August 2001).

Appendix III: Cumulative semilog grain size distribution data

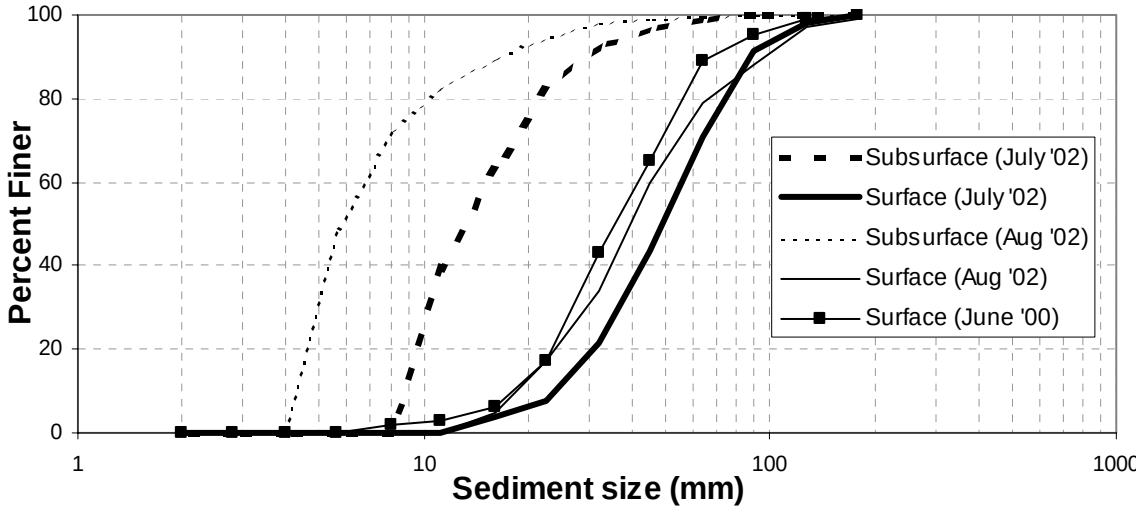

Figure A3.1 Cross section 1, bar on river right.

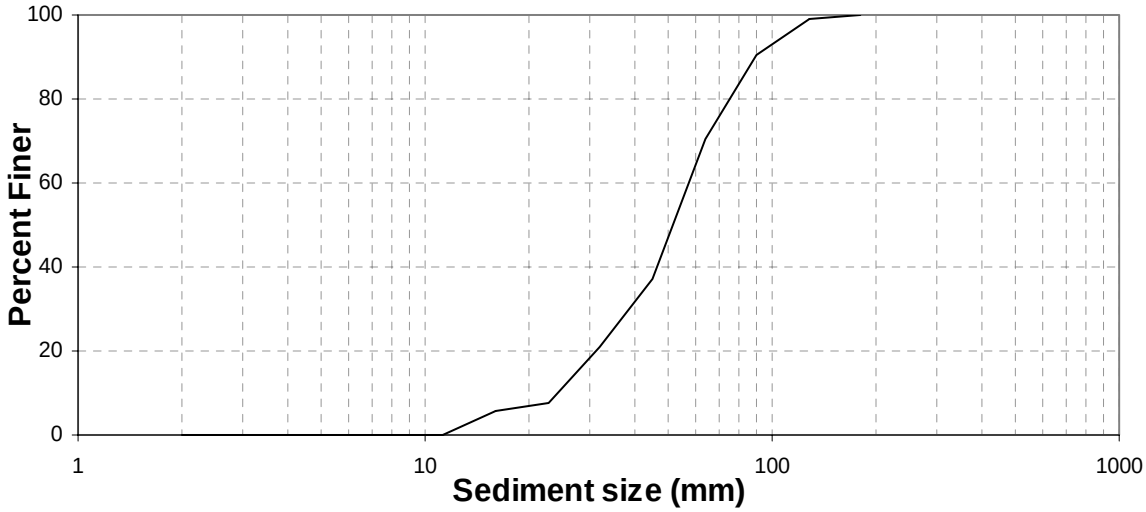

Figure A3.2 Cross section 3, bar on river right (August 2002).

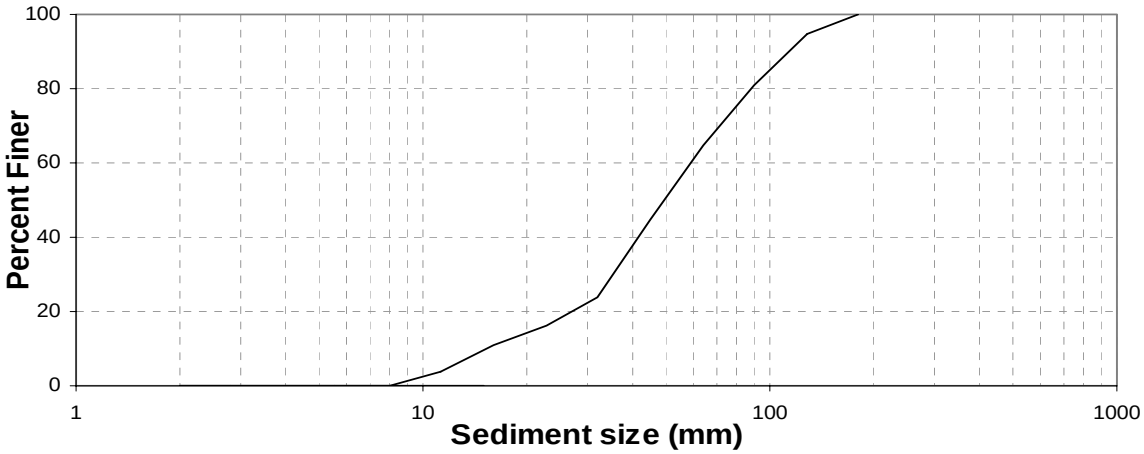

Figure A3.3 Cross section 2, bar on river left (August 2002).

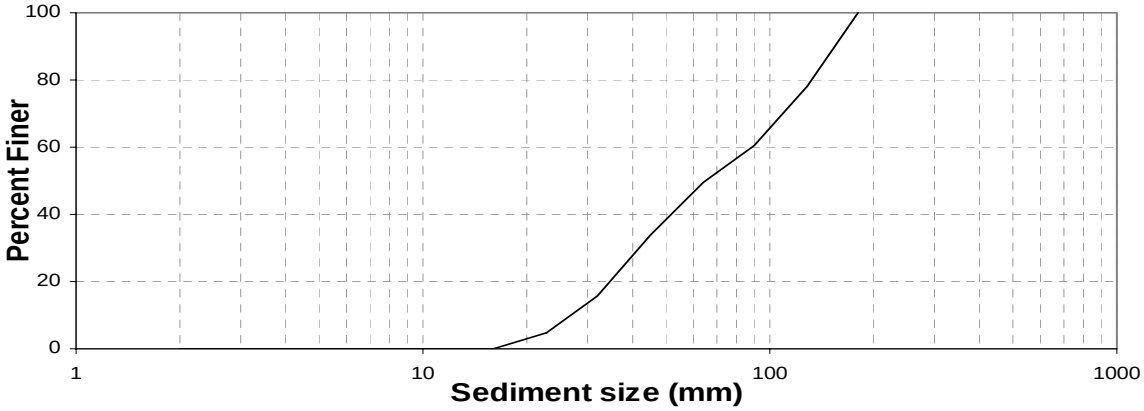

Figure A3.4 Riffle below cross section 2 (June 2000).

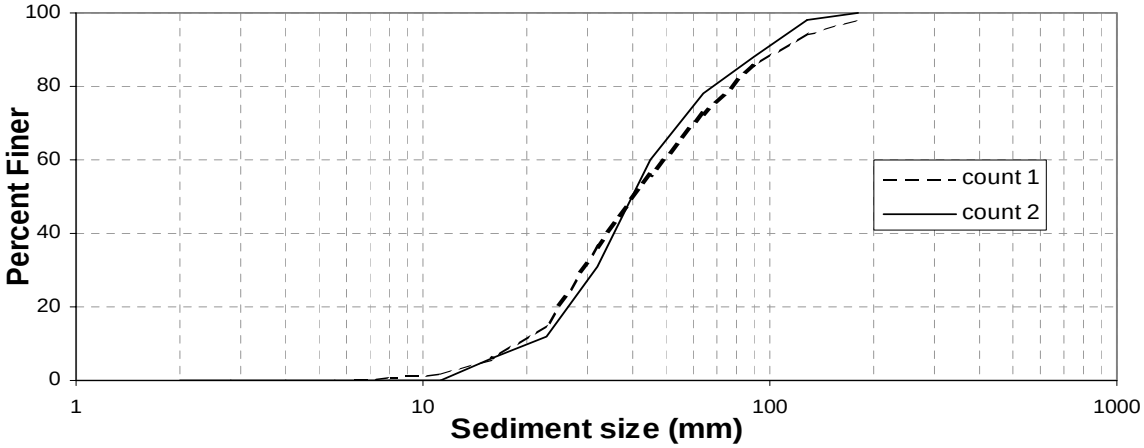

Figure A3.5 Riffle upstream from cross section 3 (June 2000).

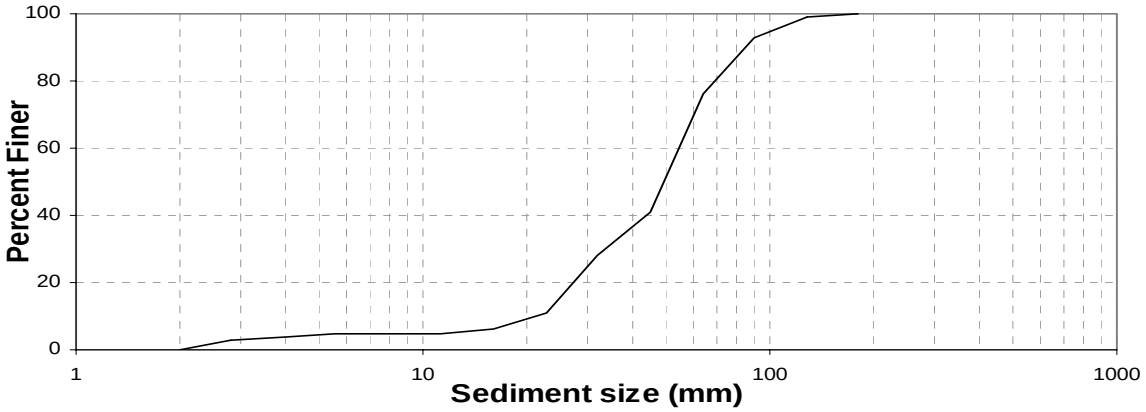

Figure A3.6 20 m downstream from cross section 3 (June 2000).

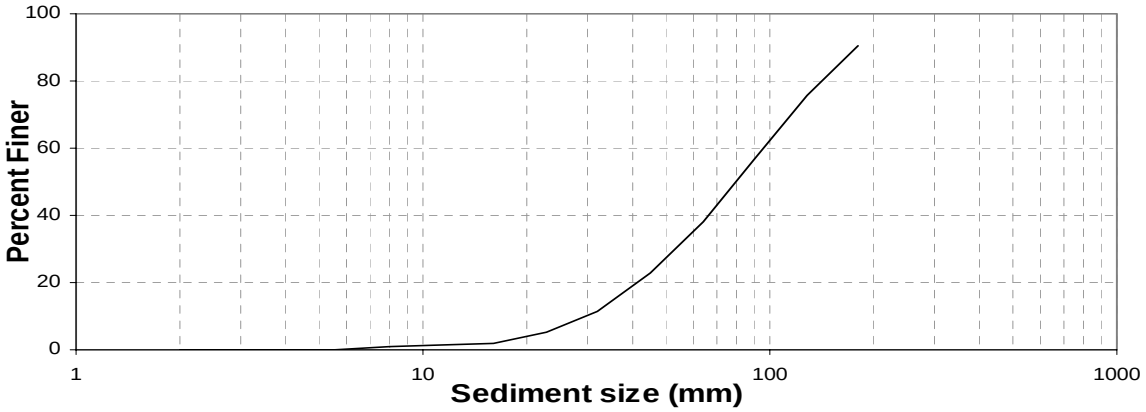

Figure A3.7 Cross section 2 (June 2001).

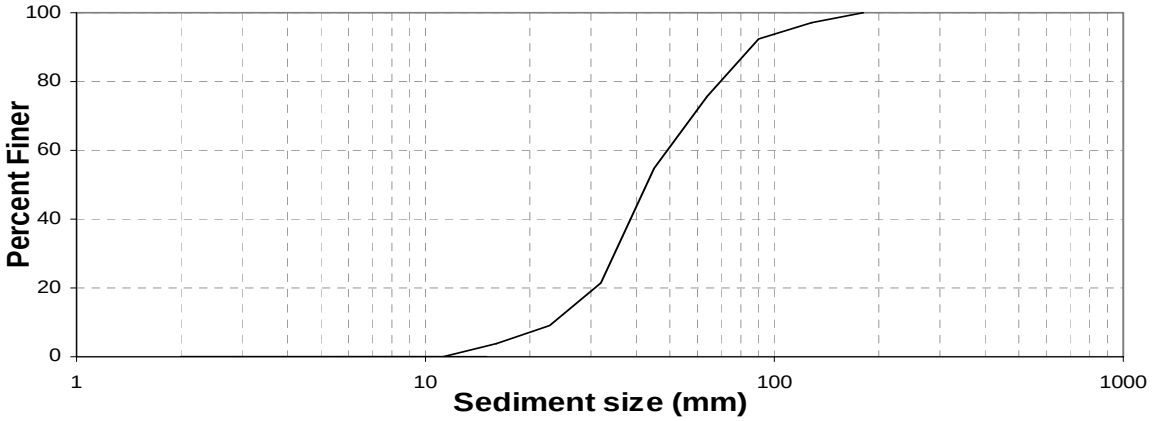

Figure A3.8 Cross Section 3 (June 2000).

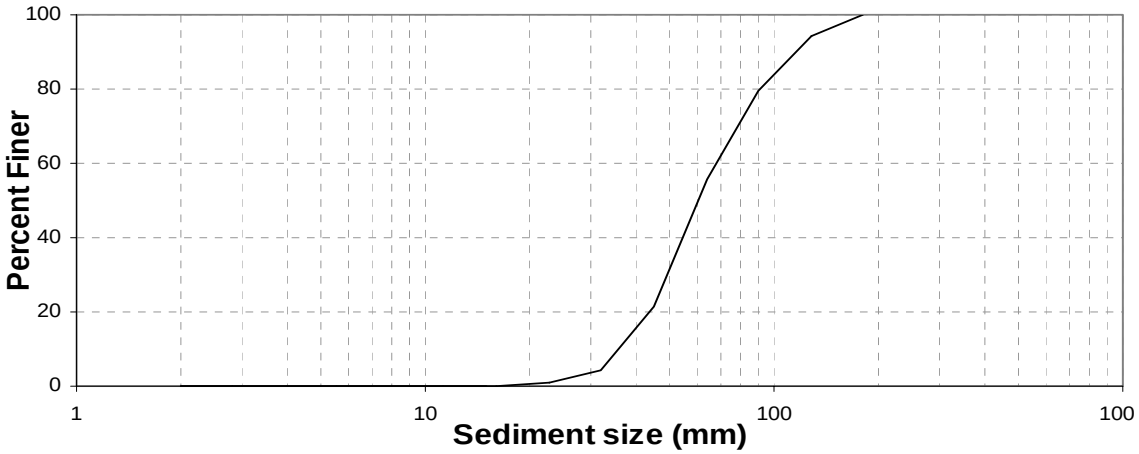

Figure A3.9 Yellow tracer rock grain size distribution.

Appendix IV: August 2002 Peak Discharge Estimation

The August 15th, 2002 event resulted in the highest stage recorded in the ten-year history of the gauge site. The rating curve for the gauge site is shown below. As this graph shows, there are very few data points above the 1-meter stage. For this reason a high water survey was performed after the flood to validate the rating curve prediction.

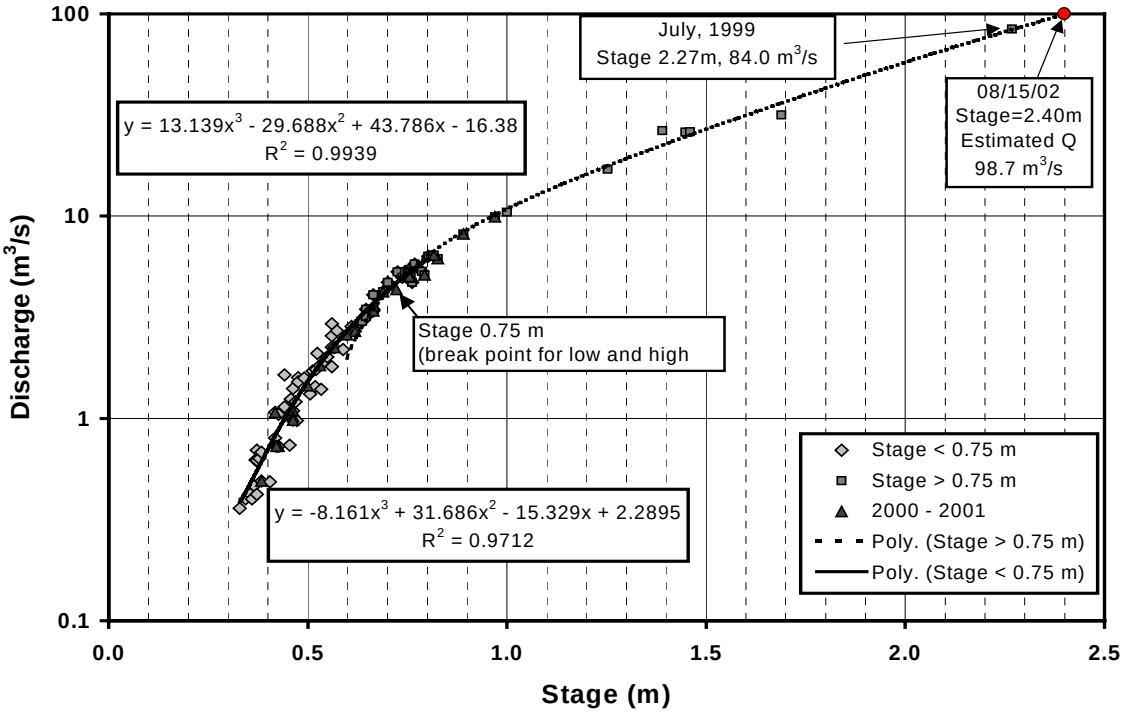

Figure A4.1 Upper Kuparuk River rating curve (Kane and Hinzman, 2002).

In the field, two cross-sections were surveyed from the high water mark on one bank to the high water mark on the other bank and the slope between the cross sections was measured. The slope-area method (Dingman, 1994) was then used to calculate the discharge.

The slope-area analysis yielded a discharge value of 93.2 m^3/s, which is in reasonable agreement with the 98.7 m^3/s predicted by the existing rating curve.

Appendix V: Channel Cross-Sections (June 2002)

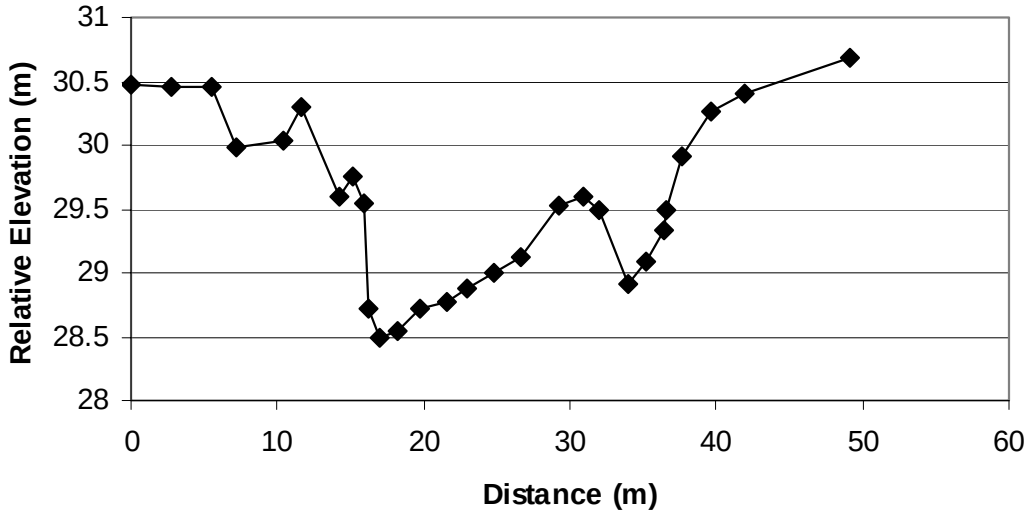

Figure A5.1 Upper Kuparuk River cross section 1.

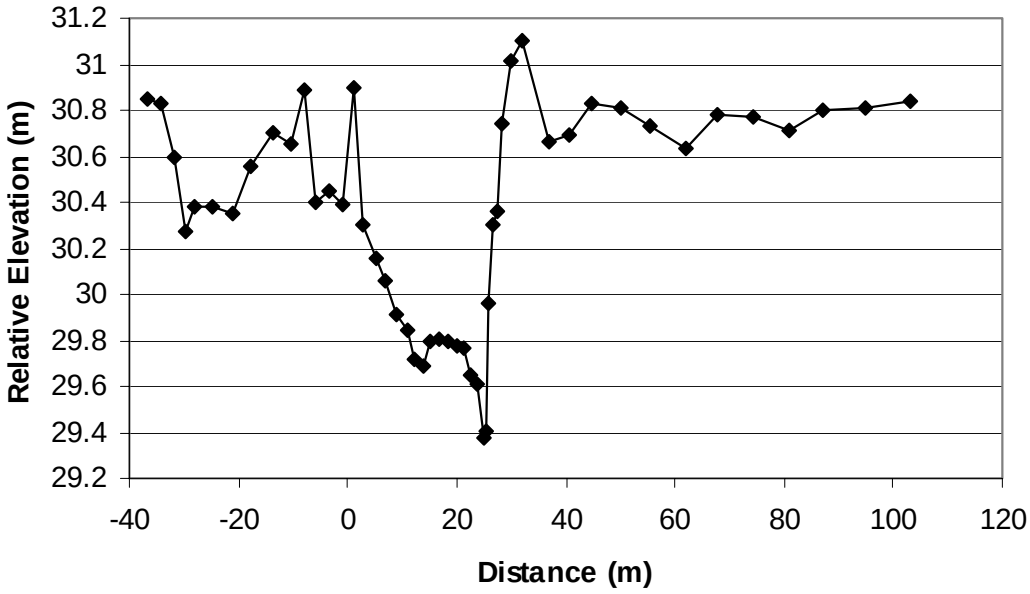

Figure A5.2 Upper Kuparuk River cross section 2.

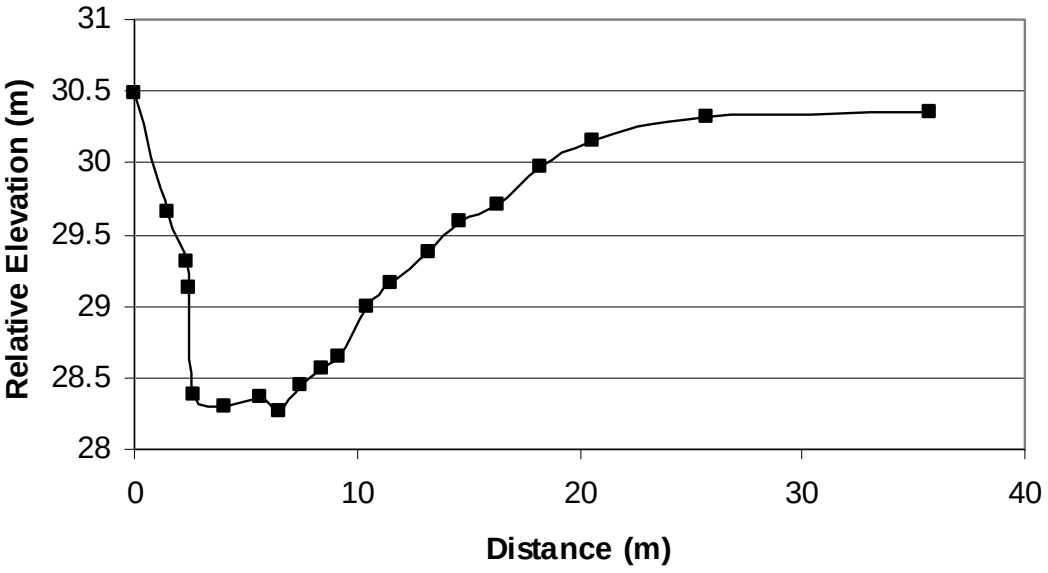

Figure A5.3 Upper Kuparuk River cross section 3.

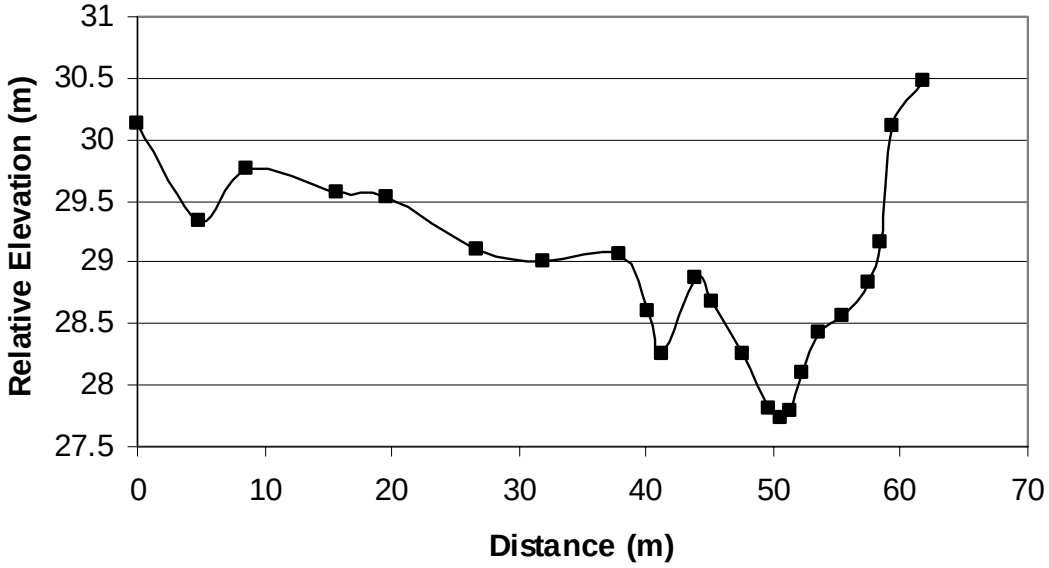

Figure A5.4 Upper Kuparuk River cross section 4.

Appendix VI: Survey Accuracy

Two consecutive surveys were performed before the event. There was no bedload transport between the times that these two surveys were performed, yet there is up to 18 cm of vertical difference between the two surveys.

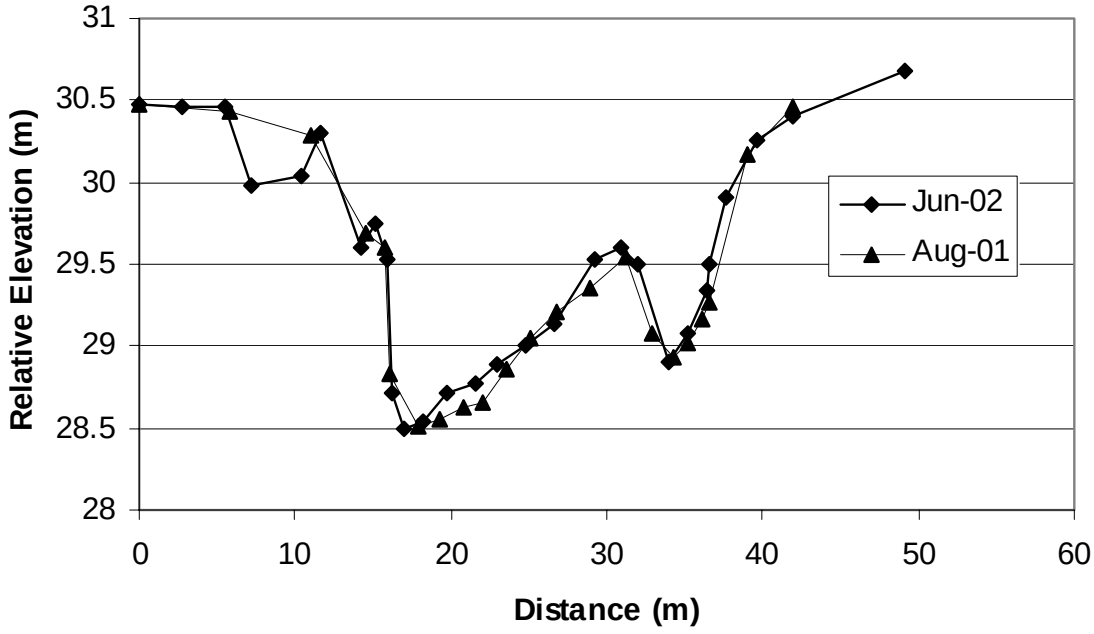

Figure A6.1 Cross Section 1 survey accuracy (pre-event).

Consecutive surveys were also performed after the event. Again, no bedload movement occurred yet there is up to 19 cm difference between the two surveys.

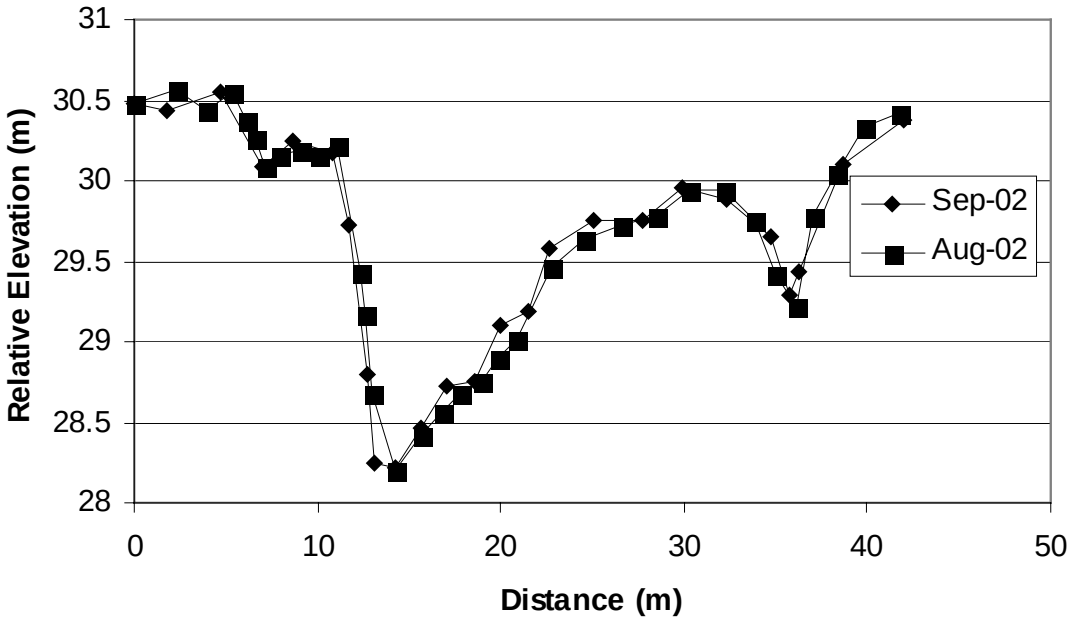

Figure A6.2 Cross Section 1 survey accuracy (post-event).

Appendix VII: Terrain Map Survey Data

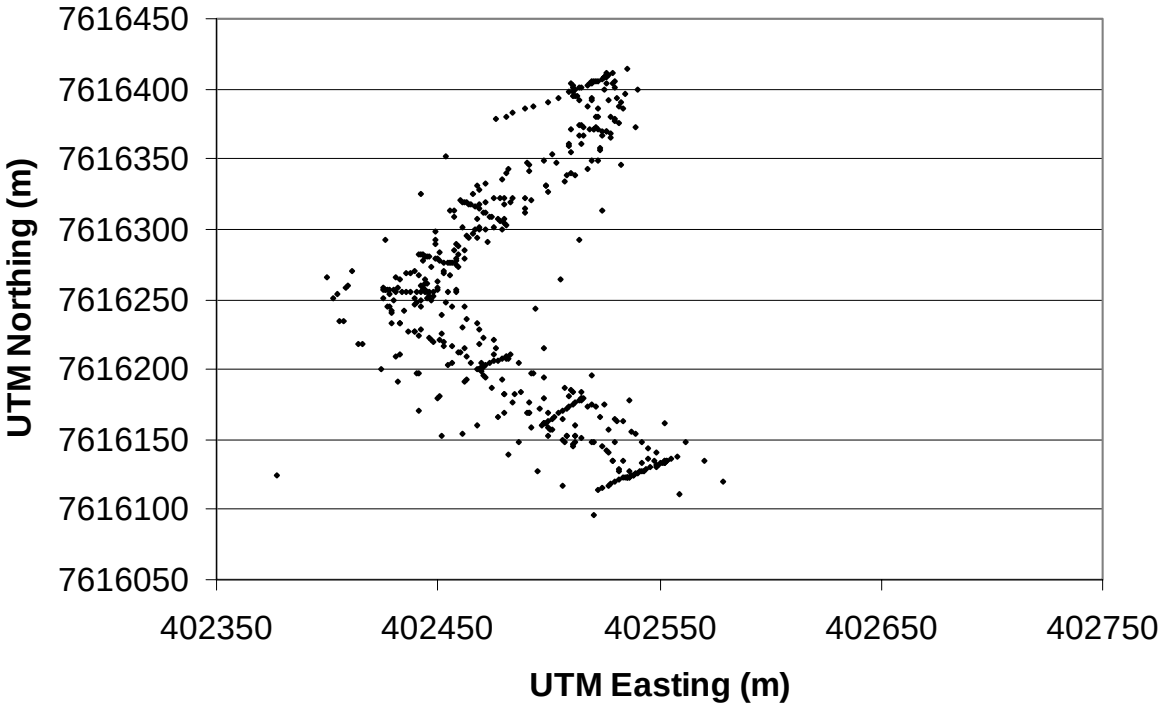

Figure A7.1 July 2002 survey grade GPS survey data set.

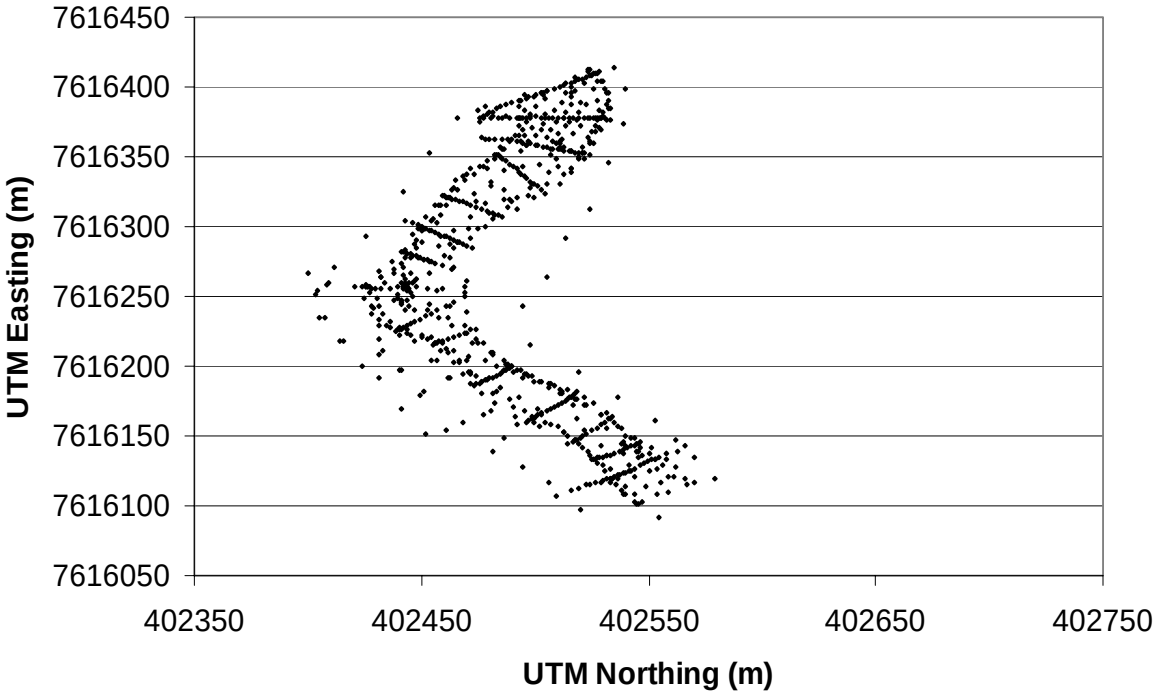

Figure A7.2 September 2002 total station survey data set.